Monthly Notices
of the
ROYAL ASTRONOMICAL SOCIETY

MNRAS **475,** 5215–5230 (2018) doi:10.1093/mnras/sty132
Advance Access publication 2018 January 15

Resonant dynamics of gravitationally bound pair of binaries: the case of 1:1 resonance

Slawomir Breiter[1]★ and David Vokrouhlický[2]

[1]*Astronomical Observatory Institute, Faculty of Physics, Adam Mickiewicz University, Sloneczna 36, PL-61-286 Poznan, Poland*
[2]*Institute of Astronomy, Charles University, Prague, V Holešovičkách 2, CZ-180 00 Prague 8, Czech Republic*

Accepted 2018 January 10. Received 2018 January 8; in original form 2017 December 8

ABSTRACT

The work presents a study of the 1:1 resonance case in a hierarchical quadruple stellar system of the 2+2 type. The resonance appears if orbital periods of both binaries are approximately equal. It is assumed that both periods are significantly shorter than the period of principal orbit of one binary with respect to the other. In these circumstances, the problem can be treated as three independent Kepler problems perturbed by mutual gravitational interactions. By means of canonical perturbation methods, the planar problem is reduced to a secular system with 1 degree of freedom involving a resonance angle (the difference of mean longitudes of the binaries) and its conjugate momentum (involving the ratio of orbital period in one binary to the period of principal orbit). The resonant model is supplemented with short periodic perturbations expressions, and verified by the comparison with numerical integration of the original equations of motion. Estimates of the binaries periods variations indicate that the effect is rather weak, but possibly detectible if it occurs in a moderately compact system. However, the analysis of resonance capture scenarios implies that the 1:1 resonance should be exceptional amongst the 2+2 quadruples.

Key words: methods: analytical – celestial mechanics – binaries: eclipsing – stars: kinematics and dynamics.

1 INTRODUCTION

The exact statistical census of stellar hierarchies, from binaries to multiple-star systems, is subject to debate because of difficulties in precise debiasing procedure of surveys. Nevertheless, a significant progress has been achieved over the past decade or so. We know that stars like companions, and nearly 10 per cent live in hierarchies of more than two (e.g. Tokovinin 2014; Riddle et al. 2015). This number was determined for solar-type stars of F- and G-classes, and it is likely quite larger for more massive stars. As outlined in Tokovinin (2008), relative number of systems with different multiplicity and their parameters (such as ratio of masses of participating stars and orbital periods of their sub-systems) put important constraints on their formation processes. These include not only direct fragmentation of the initial cloud but also orbital processes such as gas- and tide-driven migration. The latter leave important fingerprints on the presently observed architecture of the stellar systems.

In this paper, we focus on the quadruple systems. Their long-term stability requires one of the two architectures: (i) $((2 + 1) + 1)$, namely a triple system accompanied with a distant star, or (ii) $(2 + 2)$, namely two binary systems revolving about a common centre of mass. Of these two, we are concerned about the latter category (ii). Interestingly, the 2+2 systems are more frequent (e.g. Tokovinin 2008; Riddle et al. 2015) and have distinct properties, both factors suggesting their unique formation route. In particular, Tokovinin (2008) found that (i) the binaries embodied in the 2+2 quadruples are frequently composed of stars with similar mass, (ii) orbital spin of binaries and their common orbit in compact 2+2 quadruples are correlated (unlike in triples and wider 2+2 quadruples), and (iii) period ratio of the binaries in compact 2+2 quadruples is within an order-of-magnitude near unity (unlike in triples and wider 2+2 quadruples).

Unlike the primordial dynamical issues mentioned above, we deal with the present dynamical configuration. Equations of secular dynamics of quadruple systems in the 2+2 hierarchy have been formulated and studied at different levels of accuracy and with different goals (e.g. Pejcha et al. 2013; Hamers & Portegies Zwart 2016; Vokrouhlický 2016; Hamers & Lai 2017). Put in an immediate practical use, these results may be employed to interpret observations of long-term changes in architecture of these quadruple systems, such as precession of periapses of the two participating binaries or changes in orientation of their orbital planes witnessed by variations of eclipse depths (e.g. Pribulla et al. 2008; Zasche & Uhlař 2013, 2016). This is actually a traditional framework used for decades for interpretation of orbital changes in triple stellar systems, only now

★ E-mail: breiter@amu.edu.pl

adapted for a more general architecture.[1] However, as the available observational data about the 2+2 quadruple systems grow, problems of new flavor may appear. This is the case of a possibility of mean motion resonances between the two participating binary systems. Obviously, the previously developed secular approach cannot be used to tackle this problem and new tools are needed.

On the observational side, the case for such resonances has not yet been established exactly. This is because it would require a complete information about the architecture of the system. We miss such a detailed knowledge for most of the triple systems, so it is not surprising that the data about 2+2 quadruples are equally incomplete. Yet, strong hints and suggestions were recently published. For instance, Ofir (2008) suggested that the system BI 108 in the LMC field of OGLE survey is likely a doubly-eclipsing system in 2+2 architecture with orbital periods $P_{\rm A} \simeq 3.577\,98$ d and $P_{\rm B} \simeq 5.366\,55$ d for the two binaries. Ofir (2008) also noted that the periods are within $\simeq$0.03 per cent near the 3:2 ratio and conjectured that the system is in the corresponding dynamical resonant state. This commensurability of the two periods in the BI 108 system has been confirmed, and even strengthened, by Kolaczkowski et al. (2013). While discussing also other possibilities for occurrence of the two periods (see also Rivinius, Mennickent & Kołaczkowski 2011), these authors concluded that the resonant state of the two interacting binaries is the most likely conclusion. Similarly, Cagaš & Pejcha (2012) studied a double period, doubly-eclipsing system CzeV343 with $P_{\rm A} \simeq 0.806\,931$ d and $P_{\rm B} \simeq 1.209\,373$ d. Again, the ratio $P_{\rm B}/P_{\rm A}$ is within $\simeq$0.1 per cent equal to 3:2, suggestive for a dynamically resonant configuration. We also note that in both cases the longer-period orbit has been found slightly eccentric, $\simeq 0.08$ and $\simeq 0.18$. Given the first-order of the 3:2 resonance, this is a necessary pre-requisite of the physical resonance between the two binaries. On the other hand, the two systems are unresolved and, worse, the long period of the putative revolution of the centre of mass was not detected yet. It is not surprising then, that other information, such as the mutual inclination of the binary orbital planes, about the two systems is also not available.

Apart from these two strongest candidates for 3:2 resonant systems, we note that the analysis of the eclipsing binaries in the OGLE-III SMC fields by Pawlak et al. (2013) revealed 15 candidates for 2+2 quadruples. Two of them have the period ratio close to 3:2 within 1–2 per cent. Finally, we note a rare case of a doubly eclipsing unresolved Kepler system KIC 4247791. The photometric and spectroscopic analysis of Lehmann et al. (2012) revealed that it consists of two, possibly coplanar binaries on nearly circular orbits with periods $P_{\rm A} \simeq 4.04973$ d and $P_{\rm B} \simeq 4.10087$ d. This is within about a percent level close to their 1:1 ratio. However, as before, the data of this interesting system do not presently allow to reveal the mutual motion of the two binaries about their common centre of mass.

With the possible caveat that the periods in the previously mentioned systems are near-commensurate by pure chance, we take the move on the theory side and investigate conditions for mean motions resonances in the 2+2 quadruple systems. It is interesting to note that such a resonant configuration has not been studied in the past. This is for two reasons. First, as described above, the observational hints about such resonances appeared in the literature only very recently. Secondly, it has been actually customary that problems of stellar orbital dynamics were originally built on analogues from our planetary system. For instance, early studies of perturbations in triple systems were directly developed from tools of Delaunay and Hill-Brown theories of lunar motion (see Brown 1936a,b,c, 1937). In our case, however, the problem is autonomous to stellar systems and no planetary analogy exists. In this sense, while using classical tools of perturbation theory, our approach is a novel contribution to orbital mechanics.

As discussed above, the current observations motivate to study mainly the 3:2 mean motion resonance between the orbital motions of the two binaries. To set the stage and gain first insights with the problem, we however start with simpler, but also stronger, 1:1 resonance. This case requires the least analytic labour because, unlike the first-order resonances, like 3:2, it exists for circular, or near-circular, orbits of the two binaries. Unless there were reasons for the eccentricities to be triggered to large values by other dynamical effects, the resonant problem can be very well approximated with a one degree of freedom, time-independent Hamiltonian model (Sections 2 and 3). Even if the solution of the reduced model remains in formal quadratures, not being expressible in terms of elementary functions, the principal characteristics such as resonant equilibria or resonant width can be easily determined (Section 4). The model has been validated by the comparison with numerical integration of original equations of motion (Section 5), which required the addition of periodic perturbations formulae (Appendix A) and some analytical estimates of the secular evolution of eccentricities (Appendix B).

One of the most interesting aspects of the putative mean motion resonances in the 2+2 stellar quadruples is that they very likely originate from a capture (see Cagaš & Pejcha 2012). This is because the volume occupied by the resonances in the orbital phase space is extremely small. Thus, the probability that the systems happened to be born in a resonant state is very low. Rather, the resonance should have been established during the tidal evolution of $P_{\rm A}$ or $P_{\rm B}$. Therefore, the statistics of the occurrence of resonant cases could, in an ideal situation when all other biases are removed, be linked to parameters of the tidal evolution of the binary orbits. For this reason, we also pay attention to the resonant capture conditions and probability (Section 6).

2 DYNAMICAL FRAMEWORK

2.1 Variables and Hamiltonian

Consider a quadruple system made of two binary subsystems A and B (Fig. 1). The binary A includes two stars having masses m_1 and m_2, with a relative position vector $\boldsymbol{r}_{\rm A}$ directed from m_1 to m_2. Similarly, the relative position vector $\boldsymbol{r}_{\rm B}$ points from the star of the mass m_3, to the second component of the binary B, having the mass m_4. Then, the position vector $\boldsymbol{R}$ locates the centre of mass of the subsystem B with respect to the centre of mass of A. Since all three vectors are relative, they can be reckoned in any reference frame with fixed directions of axes.[2] By assumption, we attach the symbols

[1] It is interesting to note that Brown (1937), in his series of pioneering works, analysed these long-period variations for the system ξ UMa, which is actually a quadruple in the 2+2 architecture. However, one of the binary periods is much shorter than the other, so the short-period system may be conveniently replaced with a single body from the dynamical point of view and the system effectively treated as triple with sufficient accuracy.

[2] We have decided to abbreviate the notation used by Vokrouhlický (2016), replacing his subscripts Aa, Ab, Ba, Bb with 1, 2, 3, and 4, respectively, and omitting the subscript AB.

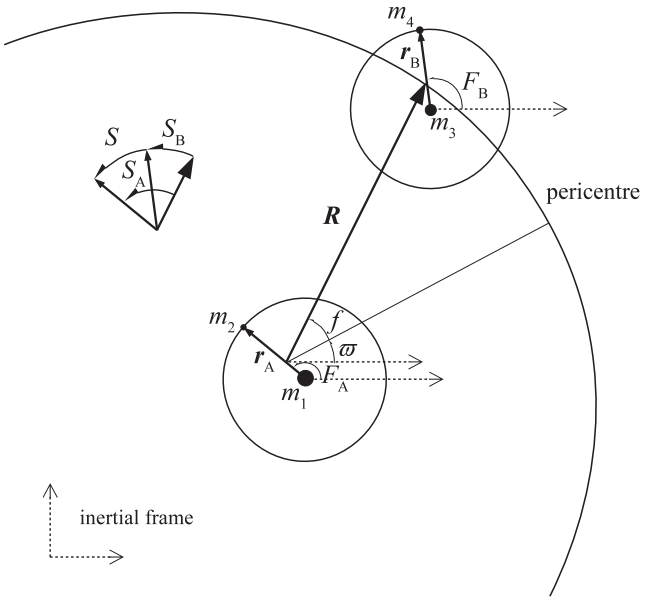

Figure 1. Geometry of the planar quadruple system. True longitudes are $F_A = f_A + \varpi_A$ and $F_B = f_B + \varpi_B$.

so that, whenever the masses are different, $m_1 > m_2$, $m_3 > m_4$, and $M_A > M_B$, where

$$M_A = m_1 + m_2, \qquad M_B = m_3 + m_4, \tag{1}$$

are the total masses of binaries A and B. With this convention, the system can be parametrized by three mass ratios

$$\mu_A = \frac{m_2}{M_A}, \quad \mu_B = \frac{m_4}{M_B}, \quad \mu = \frac{M_B}{M}, \tag{2}$$

where $M = M_A + M_B$, is the total mass of the system, with each of the coefficients belonging to the interval $(0, 1/2]$.

Attaching to $\boldsymbol{r}_A$, $\boldsymbol{r}_B$, and $\boldsymbol{R}$ momentum vectors $\boldsymbol{p}_A$, $\boldsymbol{p}_B$, and $\boldsymbol{P}$, we obtain a canonical set sometimes called 'hierarchical Jacobi coordinates' (e.g. Milani & Nobili 1983; Beust 2003). Indeed, the variables offer the advantages of the standard Jacobi variables, widespread in hierarchical triples studies, being well adapted to the hierarchy in question, having the momenta tangent to trajectories, and achieving the reduction from N to $N-1$ body problem in the canonical framework.

The Hamiltonian function of the problem, as given by Vokrouhlický (2016), may be decomposed into three distinct parts:

$$\mathcal{H} = \mathcal{H}_K\left(\boldsymbol{r}_A, \boldsymbol{r}_B, \boldsymbol{R}, \boldsymbol{p}_A, \boldsymbol{p}_B, \boldsymbol{P}\right) + \mathcal{H}_{int}\left(\boldsymbol{r}_A, \boldsymbol{r}_B, \boldsymbol{R}\right) + \mathcal{H}_c\left(\boldsymbol{r}_A, \boldsymbol{r}_B, \boldsymbol{R}\right). \tag{3}$$

The principal term

$$\mathcal{H}_K = \mathcal{H}_b + \mathcal{H}_p, \tag{4}$$

where

$$\mathcal{H}_b = \left[\frac{\boldsymbol{p}_A^2}{2\,m'_A} - G\,\frac{m'_A M_A}{r_A}\right] + \left[\frac{\boldsymbol{p}_B^2}{2\,m'_B} - G\,\frac{m'_B M_B}{r_B}\right], \tag{5}$$

$$\mathcal{H}_p = \frac{\boldsymbol{P}^2}{2\,m'} - G\,\frac{m' M}{R}, \tag{6}$$

with gravitation constant G, and reduced mass parameters

$$\begin{aligned} m'_A &= \frac{m_1 m_2}{M_A} = \mu_A(1-\mu_A)(1-\mu)M, \\ m'_B &= \frac{m_3 m_4}{M_B} = \mu_B(1-\mu_B)\mu M, \\ m' &= \frac{M_A M_B}{M} = \mu(1-\mu)M, \end{aligned} \tag{7}$$

defines three decoupled two-body problems: the motion of m_2 with respect to m_1 in the binary A, the motion of m_4 around m_3 in the binary B (both the binaries in $\mathcal{H}_b$), and the motion of the barycentre of B with respect to the barycentre of A (in $\mathcal{H}_p$) – each one following a Keplerian conic in the absence of other terms in $\mathcal{H}$.

The union of three Keplerian motions is perturbed by the interactions potential. There one may distinguish two parts: $\mathcal{H}_{int}$ and $\mathcal{H}_c$. The term

$$\begin{aligned} \mathcal{H}_{int} = &-G\,\frac{m' M}{R}\sum_{n\geq 2}\chi_{A,n}\left(\frac{r_A}{R}\right)^n P_n(\gamma_A) \\ &- G\,\frac{m' M}{R}\sum_{n\geq 2}\chi_{B,n}\left(\frac{r_B}{R}\right)^n P_n(\gamma_B), \end{aligned} \tag{8}$$

may be interpreted as defining the perturbations in a fictitious triple including the barycentre of B and the 'dipole' m_1, m_2 (first line), or in a fictitious triple system including the barycentre of A and the 'dipole' m_3, m_4 (second line). There, the Legendre polynomials P_n have arguments

$$\gamma_A = \cos S_A = \frac{\boldsymbol{R}\cdot\boldsymbol{r}_A}{R\,r_A}, \qquad \gamma_B = \cos S_B = \frac{\boldsymbol{R}\cdot\boldsymbol{r}_B}{R\,r_B}, \tag{9}$$

and the mass functions χ are

$$\begin{aligned} \chi_{A,n} &= \mu_A(1-\mu_A)\left[\mu_A^{n-1} - (\mu_A - 1)^{n-1}\right], \\ \chi_{B,n} &= \mu_B(1-\mu_B)\left[\mu_B^{n-1} - (\mu_B - 1)^{n-1}\right]. \end{aligned} \tag{10}$$

Adding either line of equation (8) to $\mathcal{H}_K$, one might obtain a typical, hierarchical three-body problem (e.g. Harrington 1969; Breiter & Vokrouhlický 2015), yet the coupling of both lines through $\boldsymbol{R}$ should not be forgotten in a non-linear approximation. But the direct coupling between all members of A and B is contained in the remainder $\mathcal{H}_c$, whose leading term reads (Hamers et al. 2015)

$$\begin{aligned} \mathcal{H}_c = &-\frac{3\,G m'_A m'_B}{4\,R}\left(\frac{r_A r_B}{R^2}\right)^2 \\ &\times\left(1 - 5\,\gamma_A^2 - 5\,\gamma_B^2 + 2\,\gamma^2 + 35\,\gamma_A^2\,\gamma_B^2 - 20\gamma\,\gamma_A\gamma_B\right), \end{aligned} \tag{11}$$

with

$$\gamma = \cos S = \frac{\boldsymbol{r}_A\cdot\boldsymbol{r}_B}{r_A\,r_B}. \tag{12}$$

The readers should be warned that the analogical equation (10) in Vokrouhlický (2016) contains an error, which makes it valid only in the planar case.

The equations of motion resulting from the Hamiltonian (3) are non-integrable, but if the binaries A and B are sufficiently distant from each other, i.e. $r_A + r_B \ll R$, we can resort to perturbation techniques, considering perturbed Kepler problems.

2.2 Preliminary simplifications

Experience suggests that mean motion related resonances are strongest when the orbits are coplanar.[3] Thus, we restrict the

[3] Moreover, observational data about the quadruples in the 2+2 hierarchy indicate near-coplanarity of many systems (e.g. Tokovinin 2008).

discussion to the planar case, where all three angular momentum vectors $\boldsymbol{r}_\mathrm{A}\times\boldsymbol{p}_\mathrm{A}, \boldsymbol{r}_\mathrm{B}\times\boldsymbol{p}_\mathrm{B}$, and $\boldsymbol{R}\times\boldsymbol{P}$ have the same direction (and their scalar products are all positive).

In the plane perpendicular to the angular momenta, the third components of the position and momentum vectors are null, and the system has 6 degrees of freedom. The angles occurring in equations (9) and (12) become related in an elementary manner:

$$S = S_\mathrm{A} - S_\mathrm{B}, \tag{13}$$

which allows to formulate equation (11) in terms of only two of the three angles.

Another simplification amounts to dropping from $\mathcal{H}_\mathrm{int}$ the terms with $n > 3$. This requires an explanation, because of an apparent inconsistence with the order of magnitude of $\mathcal{H}_\mathrm{c}$ from equation (11). By analogy with Breiter & Vokrouhlický (2015), let us introduce a small parameter ε defined by the square root of ratio of $\mathcal{H}_\mathrm{p}$ to $\mathcal{H}_\mathrm{b}$, i.e. $\varepsilon = \sqrt{\max(r_\mathrm{A}, r_\mathrm{B})/R}$. Then we have $\mathcal{H}_\mathrm{b} = O(1)$, $\mathcal{H}_\mathrm{p} = O(\varepsilon^2)$, $\mathcal{H}_\mathrm{int}(n=2) = O(\varepsilon^6)$, $\mathcal{H}_\mathrm{int}(n=3) = O(\varepsilon^8)$, and $\mathcal{H}_\mathrm{int}(n=4) = O(\varepsilon^{10})$. If the normalizing canonical transformation is sought, then non-linear terms in the Hamiltonian appear at $O(\varepsilon^9)$, as in Breiter & Vokrouhlický (2015, Section 3.1). Having decided to consider only linear perturbations in the present work, we will miss the terms of order 9, hence there is no point in considering $n = 4$ terms inside $\mathcal{H}_\mathrm{int}$, which are of order 10.

This argument, however, does not apply to $\mathcal{H}_\mathrm{c}$ – more precisely, to its resonant term amplitude. The resonance introduces a denominator of the order of the square root of the amplitude (Garfinkel 1970), which means that the effect might be $O(\varepsilon^5)$ – comparable with the influence of $\mathcal{H}_\mathrm{int}(n=2)$.

Finally, we assume that the eccentricities of unperturbed orbits in the subsystems A and B are small, although the 'principal orbit', as we are going to call the one related with $\boldsymbol{R}$, $\boldsymbol{P}$ remains elliptic. The small eccentricity assumption means that we are going to retain only the first powers of osculating e_A and e_B in the Hamiltonian, and set the mean eccentricities $e_\mathrm{A} = e_\mathrm{B} = 0$ after the averaging transformation. Let us emphasize that this particular approximation is allowed only in the 1:1 resonance case, since all other mean motion resonances, for example 3:2, require non-zero eccentricity to appear.

Having restricted the motion to the planar and almost circular case, we can introduce a subset of the modified Delaunay variables. Selecting an arbitrary departure direction in the plane of motion, we first position the pericentre of the principal orbit using the longitude of pericentre ϖ (see Fig. 1), and define the position of the barycentre of B on the orbit through the mean anomaly l. This leads to the canonically conjugate coordinate-momentum set (λ, q, Λ, Q), where

$$\begin{aligned} &\lambda = l + \varpi, \qquad \Lambda = m'\sqrt{GMa} = m'na^2, \\ &q = -\varpi, \qquad Q = \Lambda\left(1 - \sqrt{1-e^2}\right). \end{aligned} \tag{14}$$

The mean motion symbol n has a purely formal meaning, defined through $n^2a^3 = GM$, as a function of the semi-axis a; actual rate of l differs from n because of the perturbations, but we will use the term 'unperturbed principal period' for the quantity

$$P = \frac{2\pi}{n}. \tag{15}$$

For the binaries A and B, we introduce

$$\begin{aligned} &\lambda_\mathrm{A} = l_\mathrm{A} + \varpi_\mathrm{A}, \qquad \Lambda_\mathrm{A} = m'_\mathrm{A}\sqrt{GM_\mathrm{A}a_\mathrm{A}} = m'_\mathrm{A}n_\mathrm{A}a_\mathrm{A}^2, \\ &q_\mathrm{A} = -\varpi_\mathrm{A}, \qquad Q_\mathrm{A} = \Lambda_\mathrm{A}\left(1 - \sqrt{1-e_\mathrm{A}^2}\right), \end{aligned} \tag{16}$$

and

$$\begin{aligned} &\lambda_\mathrm{B} = l_\mathrm{B} + \varpi_\mathrm{B}, \qquad \Lambda_\mathrm{B} = m'_\mathrm{B}\sqrt{GM_\mathrm{B}a_\mathrm{B}} = m'_\mathrm{B}n_\mathrm{B}a_\mathrm{B}^2, \\ &q_\mathrm{B} = -\varpi_\mathrm{B}, \qquad Q_\mathrm{B} = \Lambda_\mathrm{B}\left(1 - \sqrt{1-e_\mathrm{B}^2}\right), \end{aligned} \tag{17}$$

where the osculating mean longitudes λ_A, λ_B and pericentres longitudes ϖ_A, ϖ_B are measured from the same departure direction as ϖ. The mean motions n_A and n_B are linked with the semi-axes a_A, a_B through $n_\mathrm{A}^2a_\mathrm{A}^3 = GM_\mathrm{A}$, $n_\mathrm{B}^2a_\mathrm{B}^3 = GM_\mathrm{B}$; they may serve to introduce the unperturbed periods

$$P_\mathrm{A} = \frac{2\pi}{n_\mathrm{A}}, \quad P_\mathrm{B} = \frac{2\pi}{n_\mathrm{B}}. \tag{18}$$

If f stands for the true anomaly of the principal orbit (an implicit function of all canonical variables λ, q, Λ, Q), the mutual position angles are

$$\begin{aligned} S_\mathrm{A} &= f_\mathrm{A} - f + \varpi_\mathrm{A} - \varpi, \\ S_\mathrm{B} &= f_\mathrm{B} - f + \varpi_\mathrm{B} - \varpi, \\ S &= f_\mathrm{A} - f_\mathrm{B} + \varpi_\mathrm{A} - \varpi_\mathrm{B}, \end{aligned} \tag{19}$$

where the true anomalies are functions of eccentricities and mean anomalies

$$f_\mathrm{A} = l_\mathrm{A} + 2e_\mathrm{A}\sin l_\mathrm{A} + O(e_\mathrm{A}^2),\ f_\mathrm{B} = l_\mathrm{B} + 2e_\mathrm{B}\sin l_\mathrm{B} + O(e_\mathrm{B}^2). \tag{20}$$

Expressing the Hamiltonian in these variables, we find the Keplerian part $\mathcal{H}_\mathrm{K}$ as a sum of

$$\mathcal{H}_\mathrm{b} = -\frac{(GM_\mathrm{A})^2\left(m'_\mathrm{A}\right)^3}{2\Lambda_\mathrm{A}^2} - \frac{(GM_\mathrm{B})^2\left(m'_\mathrm{B}\right)^3}{2\Lambda_\mathrm{B}^2}, \tag{21}$$

$$\mathcal{H}_\mathrm{p} = -\frac{(GM)^2(m')^3}{2\Lambda^2}. \tag{22}$$

In the truncated perturbing potential

$$\begin{aligned} \mathcal{H}_\mathrm{int} = &-G\frac{m'M}{R}\sum_{n=2}^{3}\chi_{\mathrm{A},n}\left(\frac{r_\mathrm{A}}{R}\right)^n P_n(\cos S_\mathrm{A}) \\ &- G\frac{m'M}{R}\sum_{n=2}^{3}\chi_{\mathrm{B},n}\left(\frac{r_\mathrm{B}}{R}\right)^n P_n(\cos S_\mathrm{B}), \end{aligned} \tag{23}$$

we retain the radius $R = a(1-e^2)(1+e\cos f)^{-1}$ as an exact implicit function of the canonical variables (14), whereas for the remaining two radii

$$\begin{aligned} r_\mathrm{A} &= a_\mathrm{A}(1 - e_\mathrm{A}\cos l_\mathrm{A}) + O(e_\mathrm{A}^2), \\ r_\mathrm{B} &= a_\mathrm{B}(1 - e_\mathrm{B}\cos l_\mathrm{B}) + O(e_\mathrm{B}^2). \end{aligned} \tag{24}$$

The remaining part $\mathcal{H}_\mathrm{c}$ can be transformed into

$$\begin{aligned} \mathcal{H}_\mathrm{c} = -\frac{3\,Gm'_\mathrm{A}m'_\mathrm{B}}{32\,R}\left(\frac{r_\mathrm{A}r_\mathrm{B}}{R^2}\right)^2 &(6 + 10\cos 2S_\mathrm{A} + 10\cos 2S_\mathrm{B} \\ &+ 35\cos 2(S_\mathrm{A} + S_\mathrm{B}) + 3\cos 2(S_\mathrm{A} - S_\mathrm{B})). \end{aligned} \tag{25}$$

The last term in (25) has an argument with possibly vanishing frequency, so we modify the set (16,17) introducing canonical resonance variables

$$\psi_1 = \lambda_\mathrm{A} - \lambda_\mathrm{B}, \qquad \Psi_1 = \Lambda_\mathrm{A}, \tag{26}$$

$$\psi_2 = \lambda_\mathrm{B}, \qquad \Psi_2 = \Lambda_\mathrm{A} + \Lambda_\mathrm{B}. \tag{27}$$

According to the small eccentricities postulate, for the mean variables $\psi_1 \approx S_\mathrm{A} - S_\mathrm{B}$, and $\psi_2 \approx S_\mathrm{B} + f + \varpi$, with both equalities exact if $e_\mathrm{A} = e_\mathrm{B} = 0$.

3 LINEAR SECULAR MODEL

3.1 First averaging

In the first step, we average the Hamiltonian with respect to the angle ψ_2 – the one with the presumably shortest unperturbed period. In other words, we perform a transformation of variables resulting in a partial normalization of the Hamiltonian with respect to the leading term $\mathcal{H}_\mathrm{b}$, which now reads

$$\mathcal{H}_\mathrm{b} = -\frac{(GM_\mathrm{A})^2\left(m'_\mathrm{A}\right)^3}{2\Psi_1^2} - \frac{(GM_\mathrm{B})^2\left(m'_\mathrm{B}\right)^3}{2\left(\Psi_2-\Psi_1\right)^2}. \tag{28}$$

Being more specific on the meaning of 'partial', we construct the transformation so that the new Hamiltonian belongs to the kernel of the Lie derivative

$$\mathcal{L}_2 = \frac{\partial\mathcal{H}_\mathrm{b}}{\partial\Psi_2}\frac{\partial}{\partial\psi_2} = n_\mathrm{B}\frac{\partial}{\partial\psi_2}, \tag{29}$$

instead of the complete

$$\mathcal{L}_\mathrm{b} = \frac{\partial\mathcal{H}_\mathrm{b}}{\partial\Psi_1}\frac{\partial}{\partial\psi_1} + \frac{\partial\mathcal{H}_\mathrm{b}}{\partial\Psi_2}\frac{\partial}{\partial\psi_2} = (n_\mathrm{A}-n_\mathrm{B})\frac{\partial}{\partial\psi_1} + n_\mathrm{B}\frac{\partial}{\partial\psi_2}. \tag{30}$$

Remaining in the linear approximation, we obtain the Hamiltonian in new variables through a simple averaging with respect to ψ_2. Actually, the new variables should have different symbols, but we retain the old ones and distinguish the initial, osculating set from the new 'intermediate variables' by the context. Thus, after the averaging we obtain $\overline{\mathcal{H}}_\mathrm{K}(\Psi_1,\Psi_2,\Lambda) = \mathcal{H}_\mathrm{K}(\Psi_1,\Psi_2,\Lambda)$, and,

$$\overline{\mathcal{H}}_\mathrm{int} = -\frac{GMm'}{4R}\frac{\chi_{\mathrm{A},2}a_\mathrm{A}^2 + \chi_{\mathrm{B},2}a_\mathrm{B}^2}{R^2}, \tag{31}$$

$$\overline{\mathcal{H}}_\mathrm{c} = -\frac{9\,Gm'_\mathrm{A}m'_\mathrm{B}\,a_\mathrm{A}^2a_\mathrm{B}^2}{32R^5}\cos 2\psi_1, \tag{32}$$

so that $\mathcal{L}_2\overline{\mathcal{H}} = 0$. Note that in both $\overline{\mathcal{H}}_\mathrm{int}$, and $\overline{\mathcal{H}}_\mathrm{c}$, we have set $e_\mathrm{A} = e_\mathrm{B} = 0$. Additionally, the ψ_1 independent part of $\overline{\mathcal{H}}_\mathrm{c}$ has been discarded. As a result, the intermediate $\Psi_2 = \Lambda_\mathrm{A} + \Lambda_\mathrm{B}$ becomes a new constant of motion (although both Λ_A, Λ_B, hence the semiaxes a_A, a_B, remain variable). The transformation is defined by the generating function $\mathcal{S}_1$, whose leading part, derived from $\overline{\mathcal{H}}_\mathrm{int}(n = 2)$ alone, is

$$\mathcal{S}_1 \approx \mathcal{S}_{1,\mathrm{A}} + \mathcal{S}_{1,\mathrm{B}}, \tag{33}$$

where

$$\mathcal{S}_{1,\nu} = \frac{GMm'}{8R^3}\frac{\chi_{\nu,2}a_\nu^2}{n_\nu}\left[3\sin 2(F-\lambda_\nu) - 18e_\nu\sin(2F-\lambda_\nu-\varpi_\nu) + 4e_\nu\sin(\lambda_\nu-\varpi_\nu) + 2e_\nu\sin(2F-3\lambda_\nu+\varpi_\nu)\right], \tag{34}$$

and ν stands for A or B. For brevity, we have retained the symbols λ_ν, a_ν as implicit functions of ψ_1, ψ_2, Ψ_1, and Ψ_2. The true longitude on the principal orbit is

$$F = f + \varpi. \tag{35}$$

3.2 Second averaging

The second transformation will normalize the Hamiltonian $\overline{\mathcal{H}}$ with respect to $\mathcal{H}_\mathrm{p}$, so that the new function $\overline{\overline{\mathcal{H}}}$ is independent on λ, i.e. belongs to the kernel of

$$\mathcal{L}_\mathrm{p} = \frac{\partial\overline{\mathcal{H}}_\mathrm{p}}{\partial\Lambda}\frac{\partial}{\partial\lambda} = n\frac{\partial}{\partial\lambda}. \tag{36}$$

Again, we remain within a linear perturbation theory domain, which means that the Hamiltonian in new variables is obtained through an elementary averaging with respect to λ, actually performed through the substitution rule

$$\frac{1}{2\pi}\int_0^{2\pi} Y\,\mathrm{d}\lambda = \frac{1}{2\pi}\int_0^{2\pi}\frac{YR^2}{a^2\sqrt{1-e^2}}\,\mathrm{d}f, \tag{37}$$

for any function Y explicitly depending on the true anomaly f. Thus, we find, in the new variables (named 'mean variables'), the Hamiltonian

$$\overline{\overline{\mathcal{H}}}_\mathrm{K} = \overline{\mathcal{H}}_\mathrm{K}(\Psi_1,\Psi_2,\Lambda), \tag{38}$$

$$\overline{\overline{\mathcal{H}}}_\mathrm{int} = -\frac{GMm'}{4a^3\eta^3}\left(\chi_{\mathrm{A},2}a_\mathrm{A}^2 + \chi_{\mathrm{B},2}a_\mathrm{B}^2\right), \tag{39}$$

$$\overline{\overline{\mathcal{H}}}_\mathrm{c} = -\frac{9\,Gm'_\mathrm{A}m'_\mathrm{B}\,a_\mathrm{A}^2a_\mathrm{B}^2(2+3e^2)}{64a^5\eta^7}\cos 2\psi_1, \tag{40}$$

where

$$\eta = \sqrt{1-e^2}. \tag{41}$$

In the mean variables, the system has one degree of freedom, admitting four integrals of motion: $\Lambda = \mathrm{const}$, $Q = \mathrm{const}$, $\Psi_2 = \mathrm{const}$, and $\overline{\overline{\mathcal{H}}}(\psi_1,\Psi_1,\Psi_2,\Lambda) = \mathrm{const}$. In terms of mean Keplerian elements of the principal orbit, it implies constant a and e. The generator $\mathcal{S}_2$ of the second transformation is again the sum of two similar parts

$$\mathcal{S}_2 \approx \mathcal{S}_{2,\mathrm{A}} + \mathcal{S}_{2,\mathrm{B}}, \tag{42}$$

where

$$\mathcal{S}_{2,\nu} = -\frac{GMm'\chi_{\nu,2}a_\nu^2}{4na^3\eta^3}\left(f - l + e\sin f\right). \tag{43}$$

3.3 The resonant Hamiltonian

A final fine tuning of the Hamiltonian aims at obtaining the simplest possible form. Since $\overline{\overline{\mathcal{H}}}$ actually involves two constant action variables Λ and Ψ_2, we can use their values as free parameters defining initial conditions. In particular, we are going to use Λ as a scaling parameter: dividing the momenta and the Hamiltonian by the same constant (let it be Λ) conserves the structure of canonical equations of motion, even if the transformation is not strictly symplectic (it is not univalent). Under this scaling, we introduce dimensionless momenta $J = \Psi_1/\Lambda$, $W = \Psi_2/\Lambda$, leaving the old angles under the new names, so that the variables pair to be further studied is

$$\varphi = \psi_1,\ J = \frac{\Psi_1}{\Lambda} = \frac{m'_\mathrm{A}}{m'}\sqrt{\frac{M_\mathrm{A}a_\mathrm{A}}{Ma}} = \frac{m'_\mathrm{A}}{m'}\left(\frac{M_\mathrm{A}}{M}\right)^{\frac{2}{3}}\left(\frac{P_\mathrm{A}}{P}\right)^{\frac{1}{3}}, \tag{44}$$

and, by the definition, we restrict the values of J to the range

$$0 < J \leqslant W = J + \frac{m'_\mathrm{B}}{m'}\sqrt{\frac{M_\mathrm{B}a_\mathrm{B}}{Ma}} = J + \frac{m'_\mathrm{B}}{m'}\left(\frac{M_\mathrm{B}}{M}\right)^{\frac{2}{3}}\left(\frac{P_\mathrm{B}}{P}\right)^{\frac{1}{3}}. \tag{45}$$

This scaling will be followed by the introduction of a new independent variable τ, related to time t through

$$nt = \tau, \qquad n = \frac{(GM)^2(m')^3}{\Lambda^3}, \tag{46}$$

so that $\Delta\tau = 2\pi$ is equivalent to $\Delta t = P$.

Summing up, the resonant Hamiltonian $\mathcal{K}$ is obtained from $\overline{\overline{\mathcal{H}}}$ by dropping the Ψ_1-independent part $\overline{\overline{\mathcal{H}}}_{\rm b}$, dividing the rest by factor $n\Lambda$, and substituting $\Psi_1 = J\Lambda$, $\Psi_2 = W\Lambda$, and $\psi_1 = \varphi$. The result is

$$\mathcal{K} = \mathcal{K}_0 + \mathcal{K}_2 + \mathcal{K}_4', \tag{47}$$

$$\mathcal{K}_0 = -\frac{A_{01}}{2J^2} - \frac{A_{02}}{2(W-J)^2}, \tag{48}$$

$$\mathcal{K}_2 = A_{21}J^4 + A_{22}(W-J)^4, \tag{49}$$

$$\mathcal{K}_4' = A_4 J^4 (W-J)^4 \cos 2\varphi, \tag{50}$$

where

$$\begin{aligned}
A_{01} &= \frac{(1-\mu)^2(1-\mu_{\rm A})^3\mu_{\rm A}^3}{\mu^3} = A,\\
A_{02} &= \frac{\mu^2(1-\mu_{\rm B})^3\mu_{\rm B}^3}{(1-\mu)^3} = B,\\
A_{21} &= -\frac{\mu^4}{4\eta^3(1-\mu)^2(1-\mu_{\rm A})^3\mu_{\rm A}^3} = -\frac{\mu}{4\eta^3 A},\\
A_{22} &= -\frac{(1-\mu)^4}{4\eta^3\mu^2(1-\mu_{\rm B})^3\mu_{\rm B}^3} = -\frac{1-\mu}{4\eta^3 B},\\
A_4 &= -\frac{9(2+3e^2)(1-\mu)^2\mu^2}{64\eta^7(1-\mu_{\rm A})^3\mu_{\rm A}^3(1-\mu_{\rm B})^3\mu_{\rm B}^3}\\
&= -\frac{9(2+3e^2)(1-\mu)\mu}{64\eta^7 AB}.
\end{aligned} \tag{51}$$

Introducing a constant C, defined by

$$C = \frac{\mu_{\rm B}(1-\mu_{\rm B})}{\mu_{\rm A}(1-\mu_{\rm A})}\left(\frac{\mu}{1-\mu}\right)^{\frac{5}{3}}, \tag{52}$$

we may observe that

$$\frac{W}{J} = 1 + C\left(\frac{P_{\rm B}}{P_{\rm A}}\right)^{\frac{1}{3}}, \tag{53}$$

and

$$\frac{B}{A} = C^3. \tag{54}$$

The complete equations of motion resulting from the resonant Hamiltonian $\mathcal{K}$ are

$$\begin{aligned}
\frac{{\rm d}\varphi}{{\rm d}\tau} = \frac{\partial\mathcal{K}}{\partial J} &= \frac{A_{01}}{J^3} + \frac{A_{02}}{(J-W)^3}\\
&\quad + 4A_{21}J^3 - 4A_{22}(W-J)^3\\
&\quad + 4A_4 J^3(W-J)^3(W-2J)\cos 2\varphi,
\end{aligned} \tag{55}$$

$$\frac{{\rm d}J}{{\rm d}\tau} = -\frac{\partial\mathcal{K}}{\partial\varphi} = 2A_4 J^4(W-J)^4 \sin 2\varphi. \tag{56}$$

In the next section, we analyse the properties of the resonant Hamiltonian (47) and the solution of equations (55) and (56) for the 'resonant variables' φ, J.

4 RESONANCE PROPERTIES

4.1 Equilibria

The system defined by $\mathcal{K}$ behaves in a pendulum-like manner, as seen in Fig. 4. Regardless of the mass ratios, it admits four equilibria resulting from the condition $\frac{{\rm d}\varphi}{{\rm d}\tau} = \frac{{\rm d}J}{{\rm d}\tau} = 0$. Two of them, with $\varphi = 0$, or $\varphi = \pi$, and a common value $J_{\rm u}$ are unstable. Other two, with $\varphi = \pi/2$, or $\varphi = 3\pi/2$, and the momentum $J_{\rm s}$, are stable. Thus, the motion with $\boldsymbol{r}_{\rm A}$ permanently perpendicular to $\boldsymbol{r}_{\rm B}$ (up to some presumably small periodic perturbations) is stable, whereas permanently parallel $\boldsymbol{r}_{\rm A}$ and $\boldsymbol{r}_{\rm B}$ are not.

Although in general $J_{\rm s} \neq J_{\rm u}$, a kind of degeneracy occurs when both binaries have the same total mass and the mass ratios in both binaries are equal, i.e. $\mu_{\rm A} = \mu_{\rm B}$, and $\mu = \frac{1}{2}$; we will refer to such systems as 'symmetric'. The special case of four equal masses, with $\mu_{\rm A} = \mu_{\rm B} = \mu = \frac{1}{2}$, will be called 'completely symmetric'. Symmetric systems have the ratio $C = 1$, hence $A = B$ in the coefficients of the Hamiltonian $\mathcal{K}$. According to equations (51), it means that $A_{01} = A_{02}$ and $A_{21} = A_{22}$, leading to symmetry in the coefficients of J and $(W - J)$.

In symmetric systems, the right-hand side of equation (55) becomes null at the exact value

$$J_* = J_{\rm s} = J_{\rm u} = \frac{W}{2}, \tag{57}$$

thanks to the presence of the factor $(W - 2J)$, independent of φ. According to equation (53), with $C = 1$, it means that both types of the equilibria are exactly defined by the ratio of unperturbed periods $P_{\rm B}/P_{\rm A} = 1$.

For arbitrary masses, however, the situation is less favourable: we have to face an algebraic equation of degree 13, which implies the use of approximate methods. The first approximation to the resonant values of the momentum is $J_{\rm s} \approx J_{\rm u} \approx J_*$, derived as the root of

$$\frac{\partial\mathcal{K}_0}{\partial J} = 0, \tag{58}$$

and easily found as

$$J_* = \frac{W}{1+C}. \tag{59}$$

Given the W, this value of J_* refers simply to the equal unperturbed periods $P_{\rm A} = P_{\rm B}$, as follows from equation (53). For further convenience, we can add that

$$W - J_* = \frac{CW}{1+C}. \tag{60}$$

In order to improve this estimate, we have applied a standard perturbation technique assuming that $\mathcal{K}_0 = O(1)$, $\mathcal{K}_2 = O(\varepsilon)$, $\mathcal{K}_2 = O(\varepsilon^2)$, and substituting

$$J = J_*\left(1 + \varepsilon J_1 + \varepsilon^2 J_2\right). \tag{61}$$

The parameter ε serves only for the ordering purpose and ultimately it is set to 1. The correction J_1, common for both the equilibria, is of the order of W^6

$$J_1 = \frac{4C\left(A_{21} - A_{22}C^3\right)W^6}{3A^3(1+C)^7} = \frac{C(1-2\mu)W^6}{3(1+C)^7A^2\eta^3}. \tag{62}$$

The second correction is the sum

$$J_2 = J_{\rm c} \pm J_{\rm p}, \tag{63}$$

where the first term, similar for both equilibria,

$$J_{\rm c} = \frac{C(1-2\mu)(-5+2C+7(1-C)\mu)W^{12}}{9A^4(1+C)^{14}\eta^6}, \tag{64}$$

is typically negligible. The difference between the stable and unstable equilibrium locations is given by

$$J_{\rm p} = \frac{3(1-C)C\left(2+3e^2\right)(1-\mu)\mu W^{10}}{16A^3(1+C)^{11}\eta^7}, \tag{65}$$

so that

$$J_{\rm u} \approx J_* \left(1 + J_{\rm l} + J_{\rm c} + J_{\rm p}\right), \quad J_{\rm s} \approx J_* \left(1 + J_{\rm l} + J_{\rm c} - J_{\rm p}\right), \quad (66)$$

and $J_{\rm u} - J_{\rm s} = 2J_{\rm p} \geq 0$.

As expected, all corrections vanish for symmetric systems, where either $(1 - 2\mu)$, or $(1 - C)$ become null. Readers should be warned, that the above approximations fail if the system is too compact (small W assumption violated) or if we leave the domain of stellar-type systems (e.g. abnormally large values of C when $\mu_{\rm A}$ is too small)

4.2 Libration amplitude and period

4.2.1 Oscillator and pendulum approximations

Elementary estimates of the resonance strength and time-scale can be obtained using a simple pendulum model. In order to construct it, we first introduce a shifted momentum $D = J - J_{\rm s} \approx J - J_*$, and expand $\mathcal{K}$ in Taylor series of D, dropping all powers higher than 2. Observing the orders of magnitude of subsequent terms, we retain only

$$\mathcal{K}_*(\varphi, D) = -\frac{3}{2}\left(\frac{A_{01}}{J_*^4} + \frac{A_{02}}{(W - J_*)^4}\right) D^2 + A_4 J_*^4 (W - J_*)^4 \cos 2\varphi. \quad (67)$$

The half width of the libration zone Δ (an upper bound on the amplitude of libration in J) is found by equating the Hamiltonian values with $\varphi = 0$ and $\varphi = \pi/2$, i.e. $\mathcal{K}_*(0, 0) = \mathcal{K}_*(\pi/2, \Delta)$. The result is

$$\Delta = 2J_*^4 (W - J_*)^4 \sqrt{\frac{-A_4}{3\left(A_{02} J_*^4 + A_{01}(W - J_*)^4\right)}} \approx \frac{C\, W^6}{4A\,(1 + C)^6 \eta^3} \sqrt{\frac{3\left(2 + 3e^2\right)\,(1 - \mu)\,\mu}{A\,(1 + C)\,\eta}}, \quad (68)$$

where the second line results from the substitution of equation (59). Thus, the maximum amplitude of the libration in J is directly proportional to the sixth power of W (hence to the squares of the period ratios $P_{\rm A}/P$ and $P_{\rm B}/P$).

Relating Δ to more easily observable quantities, we can use the definitions (44) and (45) to establish the rule

$$\frac{\delta P_{\rm A}}{P_{\rm A}} = 3\frac{\Delta}{J_*} = -C\,\frac{\delta P_{\rm B}}{P_{\rm B}}, \quad (69)$$

linking the amplitude of J with a relative change of period of the binary A or B.[4]

Then, the maximum relative variation of the nominal period in the binary A is

$$\frac{\delta P_{\rm A}}{P_{\rm A}} = \frac{3A^{\frac{1}{6}}}{4} \sqrt{\frac{3\left(2 + 3e^2\right)\,(1 - \mu)\,\mu}{(1 + C)\,\eta^7}} \left(\frac{P_{\rm A}}{P}\right)^{\frac{5}{3}}. \quad (70)$$

For a completely symmetric system with a circular principal orbit it simplifies to

$$\frac{\delta P_{\rm A}}{P_{\rm A}} \approx 0.36 \left(\frac{P_{\rm A}}{P}\right)^{\frac{5}{3}}. \quad (71)$$

[4] Strictly speaking, $\delta P_{\rm A}/P_{\rm A} = -C(P_{\rm B}/P_{\rm A})^{\frac{1}{3}}\,\delta P_{\rm B}/P_{\rm B}$, but in the vicinity of resonance we assume that the reference periods are equal.

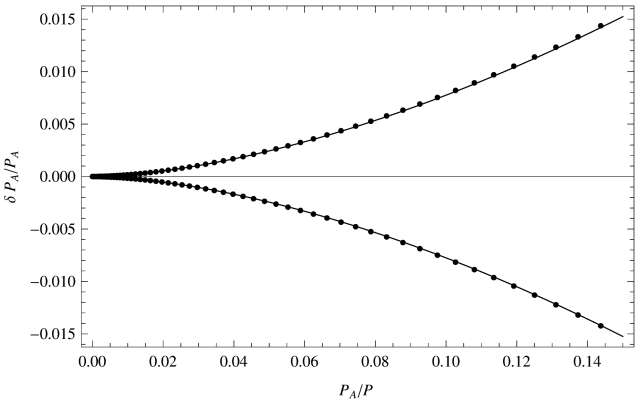

Figure 2. Maximum relative variation of period for a completely symmetric (all masses equal) system as a function of period ratio $P_{\rm A}/P$.

The minimum libration period (or the upper bound of the libration frequency) can be derived from the harmonic oscillator approximation in the vicinity of a stable equilibrium. To this end, we introduce a new angle $d = \varphi - \pi/2$ and substitute $\cos 2\varphi \approx -1 + 2d^2$ into equation (67). After dropping a constant term, we obtain the Hamiltonian

$$\mathcal{K}_{\rm h}(d, D) = -\frac{3}{2}\left(\frac{A_{01}}{J_*^4} + \frac{A_{02}}{(W - J_*)^4}\right) D^2 + 2A_4 J_*^4 (W - J_*)^4 d^2, \quad (72)$$

generating the harmonic oscillations of d and D with a frequency

$$\omega_* = \sqrt{-12A_4\left(A_{01}(W - J_*)^4 + A_{02} J_*^4\right)} \approx \frac{3}{4}\left(\frac{W}{1 + C}\right)^2 \sqrt{\frac{3\left(2 + 3e^2\right)\,(1 - \mu)\,\mu}{A\,\eta^7}}. \quad (73)$$

Recalling the time unit choice made in equation (46), we notice that the dimensionless ω_* actually gives the ratio of the principal orbit period P to the small amplitude libration period P_*, so

$$P_* = \frac{P}{\omega_*}, \quad (74)$$

regardless of the time units used in P. Thus, in particular, we have the minimum libration period

$$\frac{P_*}{P} \approx 1.37 \left(\frac{P}{P_{\rm A}}\right)^{\frac{2}{3}}, \quad (75)$$

for a completely symmetric system with $e = 0$.

4.2.2 Complete secular model

Let us confront the estimates provided in Section 4.2.1 with the numerical analysis of the complete secular equations of motion (equations 55 and 56) derived from the Hamiltonian equation (47).

In order to find the maximum relative variations of orbital periods due to the resonance, we numerically solve a system of equations

$$\begin{cases} \mathcal{K}_J(0, J_{\rm u}) = 0, \\ \mathcal{K}_J(\pi/2, J_{\rm s}) = 0, \\ \mathcal{K}(0, J_{\rm u}) = \mathcal{K}(\pi/2, J_{\rm s} + \Delta), \end{cases} \quad (76)$$

where $\mathcal{K}_J$ stands as an abbreviation for the partial derivative of $\mathcal{K}$ with respect to the momentum J. Having fixed the mass ratios and the momentum W, we find a unique quadruple ($J_{\rm s}$, $J_{\rm u}$, Δ_-, Δ_+),

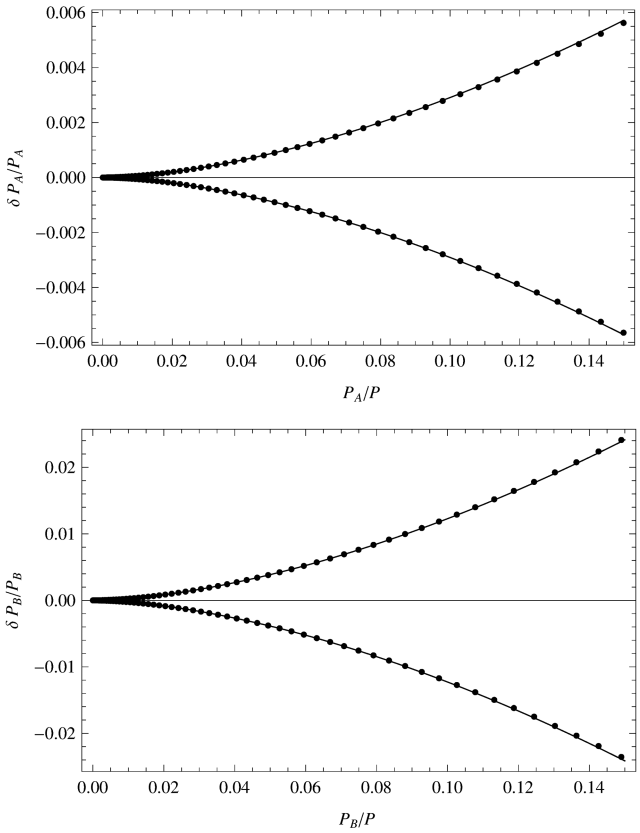

Figure 3. Maximum relative variations of periods for $m_1 = 1.70\ \mathrm{M}_\odot$, $m_2 = 1.54\ \mathrm{M}_\odot$, $m_3 = 1.46\ \mathrm{M}_\odot$, and $m_4 = 1.35\ \mathrm{M}_\odot$, as a function of period ratios P_A/P and P_B/P.

where $\Delta_\pm$ are the two real roots closest to the stable equilibrium momentum J_s: negative Δ_- and positive Δ_+. These quantities can be converted into nominal periods by means of relations

$$P_\mathrm{A}(J) = \left(\frac{\mu\, J}{(1-\mu_\mathrm{A})\,\mu_\mathrm{A}}\right)^3 \frac{P}{(1-\mu)^2}, \tag{77}$$

$$P_\mathrm{B}(J, W) = \left(\frac{(1-\mu)(W-J)}{(1-\mu_\mathrm{B})\,\mu_\mathrm{B}}\right)^3 \frac{P}{\mu^2}, \tag{78}$$

resulting from the definitions (44) and (45). Thus, with a set of solutions on some grid of the W values, we are able to trace a parametric plot with the abscissa $P_\mathrm{A}(J_\mathrm{s})/P$, and the ordinate

$$\frac{\delta P_\mathrm{A}}{P_\mathrm{A}} = \frac{P_\mathrm{A}(J_\mathrm{s}+\Delta_\pm) - P_\mathrm{A}(J_\mathrm{s})}{P_\mathrm{A}(J_\mathrm{s})}, \tag{79}$$

where the upper branch will be given by Δ_+ and the lower branch by Δ_-. Similarly, the relative variations of the binary B period are computed according to

$$\frac{\delta P_\mathrm{B}}{P_\mathrm{B}} = \frac{P_\mathrm{B}(J_\mathrm{s}+\Delta_\pm) - P_\mathrm{B}(J_\mathrm{s})}{P_\mathrm{B}(J_\mathrm{s})}. \tag{80}$$

The dots in Figs 2 and 3 represent the values obtained by this recipe. Fig. 2 refers to a completely symmetric system with all four masses equal and the eccentricity of the principal orbit $e = 0$. By symmetry, the results for δP_A and δP_B are exactly the same, save for the opposite signs, so only the plot for $\delta P_\mathrm{A}/P$ is given. In the second test case, shown in Fig. 3, the masses differ. The ratios $\mu = 0.358$, $\mu_\mathrm{A} = 0.475$, and $\mu_\mathrm{B} = 0.193$ refer to the KIC 4247791 system to be studied in Section 5. Again, the principal orbit is circular. The

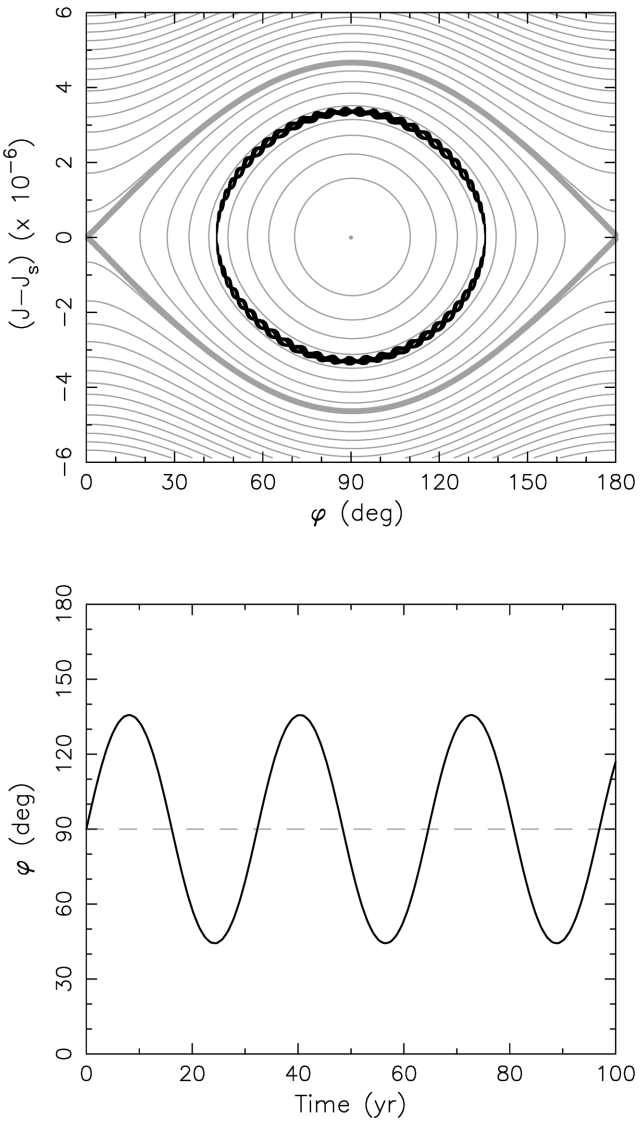

Figure 4. Top: Comparison of the numerical integration of the 1:1 resonant system (black line) with the isocontours of one-dimensional Hamiltonian $\mathcal{K}$ from equation (47) (grey lines) in the phase space of resonant variables: $\varphi = \lambda_\mathrm{A} - \lambda_\mathrm{B}$ at the abscissa and $J = \Psi_1/\Lambda$ at the ordinate ($J_* \simeq 0.0682836$ from equation 57). The bold grey line is the separatrix delimiting the 1:1 resonant zone about the stable equilibrium at $\varphi = 90^\circ$. Mean orbital elements, constructed by the procedure described in the text, are used for the numerically constructed trajectory. Bottom: Time dependence of the resonant angle $\varphi = \lambda_\mathrm{A} - \lambda_\mathrm{B}$ indicating libration period of about 32.3 yr. The initial data of the numerical run used mean orbital periods $P_\mathrm{A} = 4.0747$ d, $P_\mathrm{B} = 4.0759$ d, $P = 400$ d, zero eccentricities e_A and e_B, and the eccentricity $e = 0.25$ for the relative orbit of the two binaries. All stellar masses were set to 1.5 $\mathrm{M}_\odot$ (completely symmetric system).

maximum variation of P_B is bigger than that of P_A, because the system has a smaller mass; the ratio of amplitudes is $C^{-1} \approx 4.22$, as expected.

The numerically found values are confronted with simple estimates (71) and (70), traced as the solid lines in Figs 2 and 3, respectively. The $\frac{5}{3}$ power law holds well in both cases and the coefficients are sufficiently accurate. Of course, there is some deviation from the symmetry between positive and negative branches in the numerically computed values for the second test case, absent

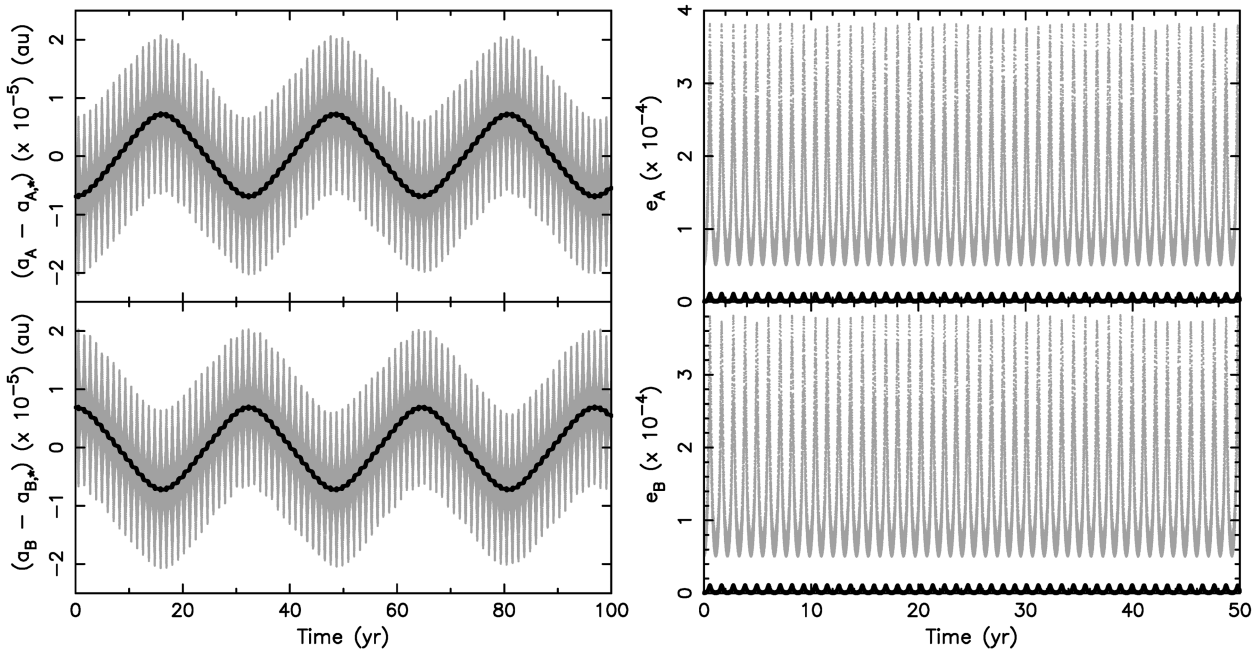

Figure 5. Semimajor axes a_A and a_B (left) and eccentricities e_A and e_B (right) for the two binaries A and B in 1:1 resonance ($a_{A,*} = a_{B,*} \simeq 0.072\,013\,65$ au). The osculating values from numerical simulation of the full-fledged problem are shown in grey. The black lines are the mean elements, semimajor axes on the left and eccentricities on the right, constructed using the analytical formulas for the quadrupole short-period effects given in the Appendix A. The mean eccentricities were constructed to be zero; their small values are due to limitations of the quadrupole corrections. The initial data of the numerical run used mean orbital periods $P_A = 4.0747$ d, $P_B = 4.0759$ d, $P = 400$ d, zero eccentricities e_A and e_B, and the eccentricity $e = 0.25$ for the relative orbit of the two binaries. All stellar masses were 1.5 $M_\odot$.

in the approximate rules (71) and (70), but it occurs on the level of at most third significant digit.

5 COMPARISON WITH FULL-FLEDGED NUMERICAL INTEGRATION

In order to justify the above-outlined theory and demonstrate it is an adequate description of the resonant motion for specific systems, we now compare its results with direct numerical integration of the complete equations of motion of a 2+2 quadruple system. The full-fledged simulation uses a Hamiltonian in the original Jacobi coordinates ($\boldsymbol{r}_A, \boldsymbol{r}_B, \boldsymbol{R}$) and the corresponding momenta ($\boldsymbol{p}_A, \boldsymbol{p}_B, \boldsymbol{P}$), in a form more general than (3) – with the potential not expanded in powers of the distance ratios. The system is propagated using the Bulrisch–Stoer method with an adaptive time step to secure high accuracy.

In the absence of the observed systems in an evident 1:1 resonance, we borrow some parameters from the study of Lehmann et al. (2012). In particular, we consider a coplanar four-body system in 2+2 architecture with orbital periods P_A and P_B near 4.0753 d, the mean of the true values observed in KIC 4247791. As expected, in order to be in the resonance, the modelled P_A and P_B need to be closer to the representative value 4.0753 d for realistic values of the outer period P. To start with, we take $P_A = 4.0747$ d and $P_B = 4.0759$ d, instead of the observed values $P_A = 4.04973$ d and $P_B = 4.10087$ d. The outer orbit period P is not known in the KIC 4247791 system, but it is possibly long. For sake of our illustration, we take $P = 400$ d. If it were longer (or even much longer), it would only mean that the resonance width is smaller, implying P_A and P_B be closer to each other. The eccentricity of the outer orbit e is 0.25, but merely the same results are obtained for all reasonably small e values (not approaching the stability limit of the quadruple system). In order to illustrate different dynamical effects, we find it interesting to first consider an equal-mass situation before we compare its results with the cases where the best-fitting stellar masses from Lehmann et al. (2012) are used. Specifically, we start with a situation where all four masses of the stars in A and B systems are 1.5 $M_\odot$.

Our aim is to consider binary orbits with zero mean eccentricities e_A and e_B. However, we know the mutual interactions necessarily excite small eccentricity values. At this moment, it is useful to recall the relation between the mean and osculating orbital elements, briefly outlined in the Appendix A. Each of the orbital elements $\boldsymbol{e} = (a_A, k_A, h_A, \lambda_A; a_B, k_B, h_B, \lambda_B; a, K, H, \lambda)$ is subject to the short-period perturbations $\delta\boldsymbol{e}$. The osculating values $\boldsymbol{e}_o$ are thus composed of the mean values $\boldsymbol{e}_m$ and $\delta\boldsymbol{e}$: $\boldsymbol{e}_o = \boldsymbol{e}_m + \delta\boldsymbol{e}$. What we aim to work with, and compare to the simple Hamiltonian theory of the resonance, are the mean elements $\boldsymbol{e}_m$. For instance, the orbital periods P_A, P_B, P (and the related semimajor axes), or the eccentricity e mentioned above are the initial mean values. The same way, our intended mean values of both e_A and e_B are zero. But to practically set the initial conditions of our numerical run, we need the initial osculating values of the elements and from them the Jacobi coordinates and momenta. Therefore, we need to add $\delta\mathbf{e}$ to our specified values of periods/semimajor axes and eccentricities. These corrections have been worked out in the Appendix A. To make the situation simplest, we use the initial mean $\lambda_A = 180°$, $\varpi_A = 0°$, $\lambda_B = 90°$, $\varpi_B = 90°$, $\lambda = 90°$, and $\varpi = 270°$. In this configuration, the correction of secular angles (ϖ_A, ϖ_B, ϖ) are zero, and only eccentricities are given small non-zero values (e.g. $e_A = \delta k_A$ from equation A6 and $e_B = \delta h_B$ from equation A7). Additionally, the longitudes λ_A and λ_B are such that the system starts with the resonant angle $\varphi = 90°$, corresponding to the stable equilibrium if $J = J_s$, or to the maximum difference between J and its

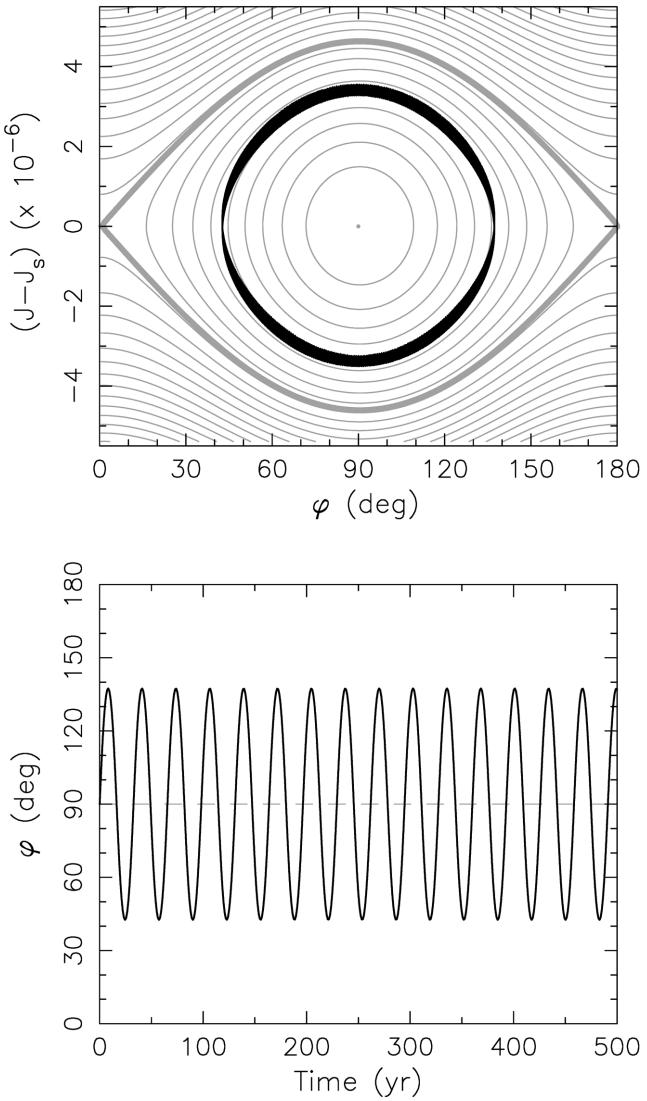

Figure 6. The same as in Fig. 4, but now for a 2+2 system with the same masses as in the KIC 4247791 system: $m_1 = 1.70\ \mathrm{M}_\odot$, $m_2 = 1.54\ \mathrm{M}_\odot$, $m_3 = 1.46\ \mathrm{M}_\odot$, and $m_4 = 1.35\ \mathrm{M}_\odot$ (see Lehmann et al. 2012). The reference level for the resonant momentum is now $J_* \simeq 0.0767632$ (top panel).

equilibrium value J_s on a given orbit, which is actually the case. The short-period corrections to the principal orbit elements are less important, but also available in the Appendix (Section A2).

Setting the initial data, we numerically propagated the complete system for time interval of 200 yr, outputting the Jacobi state vectors ($\boldsymbol{r}_\mathrm{A}, \boldsymbol{r}_\mathrm{B}, \boldsymbol{R}; \boldsymbol{p}_\mathrm{A}, \boldsymbol{p}_\mathrm{B}, \boldsymbol{P}$) every 6 hr. These were straightforwardly used to compute osculating orbital elements $\boldsymbol{e}_\mathrm{o}$. However, as we need to compare the mean, rather than osculating, orbital elements to the analytical theory from Sections 3 and 4, we subtracted the short-period perturbations $\delta\boldsymbol{e}$ provided in the Appendix A to obtain the mean orbital elements $\boldsymbol{e}_\mathrm{m}$. Finally, the mean resonant variables J and φ are computed using the mean orbital elements. The momentum J was evaluated from a_A and a, according to equation (44), and φ as a difference $\lambda_\mathrm{A} - \lambda_\mathrm{B}$.

Figs 4 and 5 show the results. In the top part of Fig. 4, we compare the phase-space trajectory of the numerically determined resonant variables (φ, J) (black line) with the isocountours of the resonant Hamiltonian $\mathcal{K}$ from equation (47). The correspondence is very good, implying the resonant Hamiltonian is an adequate model of the 1:1 resonance in this case. The small wiggles in the numerical solution reflect imperfection in our construction of the mean orbital elements, most likely because formulas for $\delta\mathbf{e}$ use only the quadrupole short-period corrections. Both panels of Fig. 4 show that the resonant angle φ librates about the equilibrium at 90° with an amplitude of nearly 45°. The libration period is $\simeq$32.3 yr, which favourably compares with the simple lower limit estimate $\simeq$ 27.4 yr from equations (73) and (74). The slightly longer value is due to finite, and non-negligible, amplitude of libration. Because the initial conditions were at $\varphi = 90°$, the difference of the initial mean periods P_A and P_B from their average value $\bar{P}_\mathrm{A} = \bar{P}_\mathrm{B} \simeq 4.0753$ d quantitatively characterizes the possible extent of the resonant state. We find $(P_\mathrm{A} - \bar{P}_\mathrm{A})/\bar{P}_\mathrm{A} \simeq 1.47 \times 10^{-4}$. Indeed, the resonance width $\Delta \simeq 4.65 \times 10^{-6}$ (see the top panel of Fig. 4), so that $3\Delta/J_* \simeq 2.03 \times 10^{-4}$. Using equation (69), we note that the fractional difference of the initial mean periods from their mean may be increased by about 35 per cent to remain possibly locked in the 1:1 resonance, but not more. As a result, the maximum fractional difference in periods P_A and P_B to characterize the resonant case is $\simeq 4 \times 10^{-4}$, far smaller than $\simeq 1.2 \times 10^{-2}$. Therefore, assuming the relative orbit of the binaries A and B has a period of a year or longer, the system KIC 4247791 is near, but not in the 1:1 mean motion resonance.

Fig. 5 shows time dependence of the semimajor axes and eccentricities of the binaries A and B. The grey symbols are the osculating elements, the black symbols are the mean elements resulting from subtraction of the short-period terms. As expected from equation (A3), the short-period effects in semimajor axes a_A and a_B have the shortest periods $\simeq P_\mathrm{A}$ and $\simeq P_\mathrm{B}$, but their amplitude is the largest when the outer orbit is at pericentre (this is because of the $\propto (a/R)^3$ factor in equation A3). The short-period effects in the eccentricities e_A and e_B have primarily the period P of the outer orbit; this is because of the constant term in the square-root factor in equation (A8). The mean values of the semimajor axes fairly well follow the short-period-averaged trend of the osculating values and oscillate with the period of $\simeq$32.3 yr. This is obviously the libration, resonant term. Its amplitude is about the same as that of the short-period effects in this case. The mean eccentricities of both A and B orbits remain very small, less than $\simeq 1.2 \times 10^{-5}$. Their non-zero values reflect a slight inadequacy of our formulas for the short-period perturbations, perhaps because contribution of higher-order than quadrupole terms near the pericentre of the outer orbit.

Figs 6 and 7 show the same as Figs 4 and 5, but now from a numerical run where we used non-equal masses of the four stars in systems A and B (otherwise, all initial data were the same). In particular, we used the best-fitting values $m_1 = 1.70\ \mathrm{M}_\odot$, $m_2 = 1.54\ \mathrm{M}_\odot$, $m_3 = 1.46\ \mathrm{M}_\odot$, and $m_4 = 1.35\ \mathrm{M}_\odot$ from Lehmann et al. (2012). As it is typical for the quadruple systems in 2+2 hierarchy, the masses are unequal, but not significantly different. Fig. 6 shows that the resonant dynamics are not affected by such a small change in masses of participating stars. However, a difference is seen in the behaviour of eccentricities e_A and e_B in the right-hand panels of Fig. 7 (the semimajor axes a_A and a_B are again basically the same as before). This change with respect to the idealized equal-mass case considered above is due to the activation of the octupole term in the secular coupling of the two binaries ($n = 3$ term in equation 23). The octupole term is well known to excite the eccentricities (see the Appendix B and Vokrouhlický 2016). Luckily, the effect is quite small in our case due to two effects: (i) the mass parameters μ_A and μ_B are not much different from one half, such that the octupole strength factors $1 - 2\mu_\mathrm{A}$ and $1 - 2\mu_\mathrm{B}$ are small,

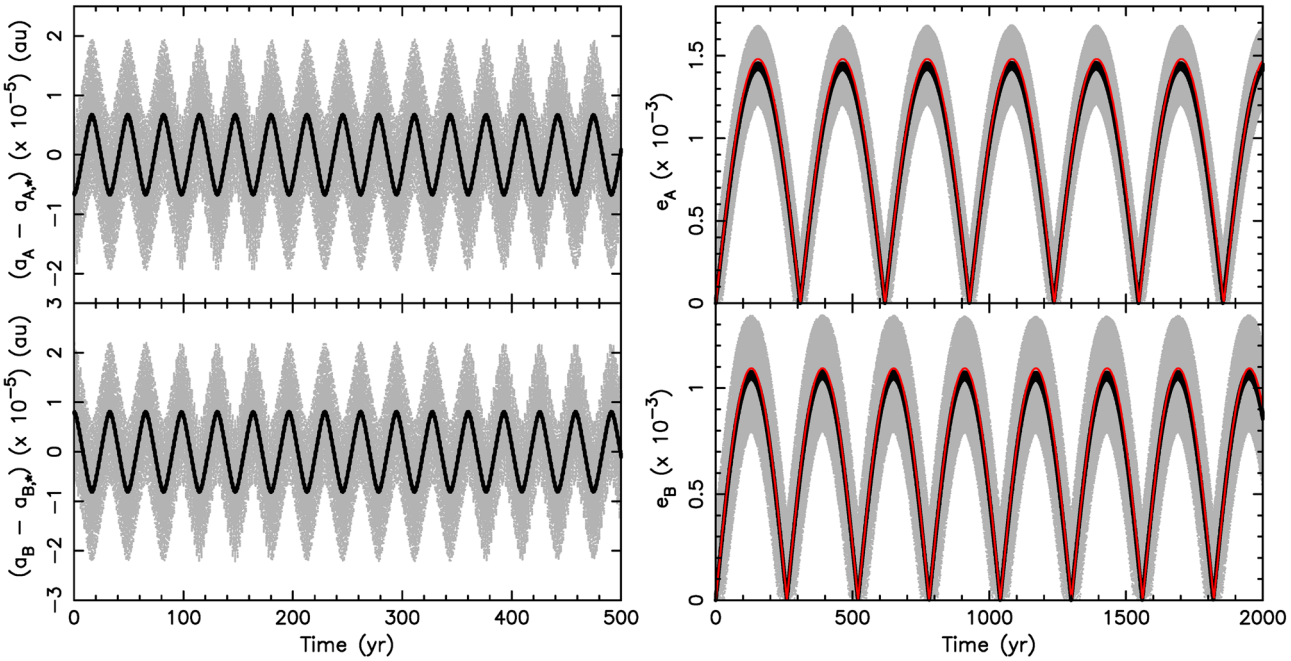

Figure 7. The same as in Fig. 5, but now for a 2+2 system with the same masses as in the KIC 4247791 system: $m_1 = 1.70\ M_\odot$, $m_2 = 1.54\ M_\odot$, $m_3 = 1.46\ M_\odot$, and $m_4 = 1.35\ M_\odot$ (see Lehmann et al. 2012). The reference semimajor axes are now $a_{A,\star} \simeq 0.073\,8842$ au and $a_{B,\star} \simeq 0.070\,4590$ au. Non-equal masses in the binaries activate the secular octupole interaction. The principal consequence is the secular perturbation of the eccentricities e_A and e_B as described in the Appendix B. The black curves are again the mean eccentricities determined by our procedure of quadrupole short-period perturbation subtraction from the osculating values; red is our simplified solution (equation B10).

and (ii) the system is not too compact, namely the fraction $a_A/a \simeq a_B/a \simeq 0.037$ is small (generally the factor by which multipolar terms decrease). This implies that the simple approximation developed in the Appendix B provides fairly accurate result. Indeed, the mean eccentricities of the A and B systems, constructed as usual by subtracting the short-period terms from the osculating values (black symbols in Fig. 7), are rather well matched by the prediction (equation B10) from our simple theory outlined in the Appendix B. The agreement will obviously become less satisfactory for more compact quadruple systems, P/P_A smaller, and/or cases with larger differences masses of participating stars, $1 - 2\mu_\nu$ larger.

Our previous analysis showed that making the system more compact, namely assuming P smaller, would increase the resonant width. Thence, a question arises – possibly of a theoretical, rather than realistic nature – whether it could increase enough to match the orbit periods observed in the KIC 4247791 system. For sake of a test, we thus re-ran our previous simulation with the following modification: (i) the orbital periods of binaries A and B were set $P_A = 4.100\,871$ d and $P_B = 4.049\,732$ d (those observed in the KIC 4247791 system Lehmann et al. 2012), and (ii) assumed the principal orbit with period $P = 45$ d and eccentricity $e = 0.1$. Note that this period is well above the limit required for the long-term stability of the system (e.g. Mardling & Aarseth 2001; Sterzik & Tokovinin 2002). Again, all stellar masses are as in the KIC 4247791 system. Results are shown in Figs 8 and 9. Libration of the resonant angle φ (Fig. 8) indicates that the system is locked in the resonance. In our example, the libration amplitude is quite large, but pushing P to still smaller values could make the libration amplitude smaller. The libration period now decreased to $\simeq$1.37 yr, as expected from a very compact quadruple system. Since the system remains in the 1:1 resonance, the semimajor axes a_A and a_B show the same pattern as before, but the e_A and e_B are different. Quite stronger coupling of the two binaries now implies that the amplitude of the short-period effects is $\simeq$0.025. This is larger than the forced eccentricity due to secular octupole coupling, which explains why the secular pattern is not seen this time. Still, the eccentricities e_A and e_B remain small enough.

We conclude that the observed orbital periods and stellar masses reported for the system KIC 4247791 are not incompatible with the 1:1 mean motion resonant state as such (assuming coplanarity). However, the orbital period of their relative motion would need to be short enough ($\leq$45 d, say). It is to be seen if this requirement is not in conflict with other observational data of this interesting system. For instance, the very similar value of the systemic velocities of the A and B systems reported by Lehmann et al. (2012) imply very likely a quite longer period P. It is also not clear whether the short P value would not produce unobserved eclipse time variations in the Kepler photometry. So our simulation demonstrates a possibility of a system to be locked in a 1:1 resonance even with about a per cent-level difference in periods P_A and P_B, but it would actually apply only if other observational facts corroborate this model (unlikely in the case of KIC 4247791 system).

6 RESONANCE CAPTURE DISCUSSION

A fundamental question concerning a resonance is the presence or absence of some mechanism locking the system in such a particular state. Without a capture mechanism, resonance may only appear randomly, like a winning lottery ticket, or as a temporary phase of evolution, like a particular number in a long countdown. Since the systems in a 1:1 resonance do not seem to be prolific amongst quadruple systems, let us inspect the problem according to the classical scenario discussed by Henrard (1982).

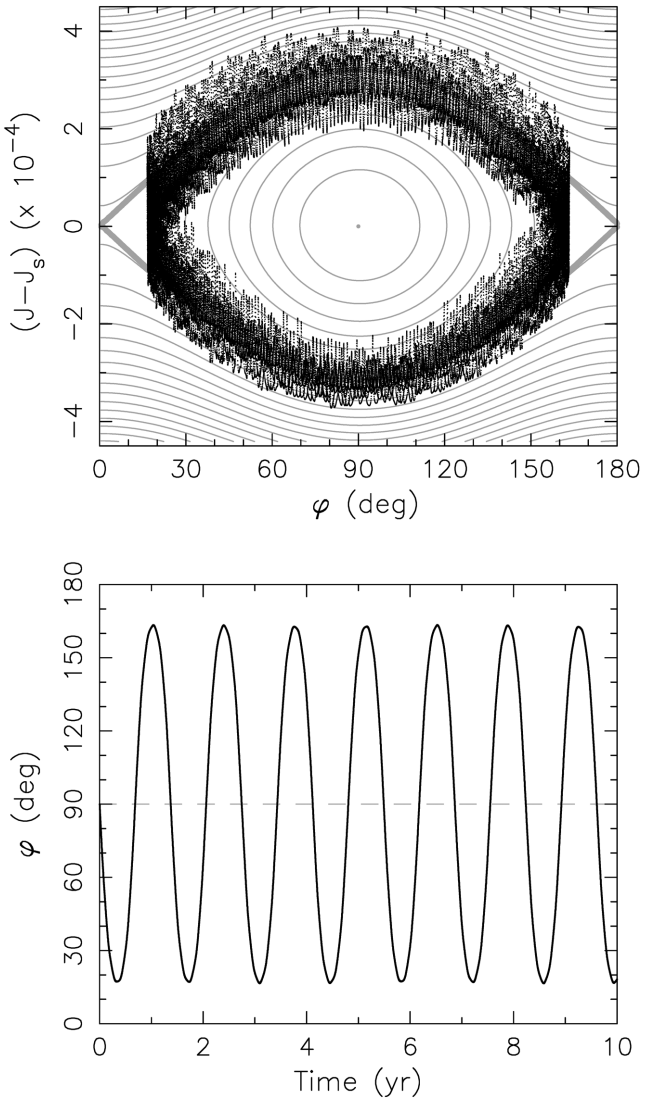

Figure 8. The same as in Fig. 6, but now for a 2+2 system with the same masses and orbital periods as in the KIC 4247791 system: $m_1 = 1.70\ \mathrm{M}_\odot$, $m_2 = 1.54\ \mathrm{M}_\odot$, $m_3 = 1.46\ \mathrm{M}_\odot$, $m_4 = 1.35\ \mathrm{M}_\odot$, $P_\mathrm{A} = 4.100\,871$ d, and $P_\mathrm{B} = 4.049\,732$ d (see Lehmann et al. 2012). The relative orbit has been given a period $P = 45$ d and eccentricity $e = 0.1$. The reference level for the resonant momentum is now $J_* \simeq 0.159\,0715$ (top panel).

Similarly to Henrard, we are going to use a one degree of freedom Hamiltonian with a slowly varying parameter, which makes the system non-conservative, yet amenable to adiabatic approximation. For the qualitative discussion, we can use the pendulum-like Hamiltonian (67) with two modifications: the momentum D is replaced with an explicit form $(J - J_*)$, and the approximate value (59) is substituted in all occurrences of J_*. The result is

$$\mathcal{K}_\star(\varphi, J; W) = \frac{\alpha}{W^4}\left(J - \frac{W}{1+C}\right)^2 + \beta W^8 \cos 2\varphi, \tag{81}$$

where W-independent coefficients are

$$\alpha = -\frac{3}{2}\frac{(1+C)^5 A}{C}, \quad \beta = \frac{C^4 A_4}{(1+C)^8}. \tag{82}$$

Further, let us assume that W, is the slowly varying parameter of the Henrard's model, with $\dot{W} = \text{const}$. Since all other parameters (in particular the mass ratios) are held fixed, the drift of W must be related to secular change of the orbital period P_B in equation (45).

At this point, we have to admit that technically the variability of W as one of the canonical variables and not a physical parameter is to some extent an abuse of the Henrard's model, because it implies the action of some force not having a potential function (so, impossible to include in the Hamiltonian function). But the essence of heuristic reasoning shown below is more general and actually agrees with numerical tests we performed to validate the conclusions (numerical integration of equations 55 and 56 with a slowly varying W).

According to Henrard (1982), the fate of motion, once it gets close to the separatrix region, is determined by the values of energy increments accumulated during the motion in the close neighbourhood of an upper separatrix (the values of momentum $J_* < J \leq J_* + \Delta$) and its lower counterpart ($J_* - \Delta \leq J < J_*$). Since both values can be well approximated by the integrals along the separatrices, we need a separatrix equation, giving J as a function of φ, W, and the Hamiltonian value $E_\star = \mathcal{K}_\star(0, W/(1+C); W) = \beta W^8$. Solving a simple quadratic equation $\mathcal{K}_\star(\varphi, J; W) = E_\star$ for J, one easily finds

$$J_\pm = \frac{W}{1+C} \pm \sqrt{\frac{2\beta}{\alpha}}\, W^6 |\sin\varphi|. \tag{83}$$

Then, the resulting energy increments are

$$B_1 = -\dot{W}\int_\pi^0 \frac{\partial J_+}{\partial W}\mathrm{d}\varphi = \dot{W}\left(\frac{\pi}{1+C} + 12\sqrt{\frac{2\beta}{\alpha}}\, W^5\right), \tag{84}$$

for the upper separatrix motion, and

$$B_2 = -\dot{W}\int_0^\pi \frac{\partial J_-}{\partial W}\mathrm{d}\varphi = \dot{W}\left(-\frac{\pi}{1+C} + 12\sqrt{\frac{2\beta}{\alpha}}\, W^5\right), \tag{85}$$

for the lower separatrix. Compared to the original B_i definition of Henrard (1982), our integration limits differ in two aspects. First, having 2φ in the Hamiltonian (81), we integrate over the interval of the length π, which is a minor issue. More important is the swap of the upper and lower limits that adjusts to the opposite direction of motion along the upper and lower separatrices with respect to the Henrard's model. The readers should note that Henrard considered the case, where the stable equilibrium is the local minimum of the Hamiltonian function, whereas the stable equilibrium at $\varphi = \pi/2$ is the maximum of our $\mathcal{K}_\star$, which implies a different reasoning based on the signs of B_1 and B_2.

Consider the decrease of P_B as an expected outcome of tidal interactions (or another dissipative mechanism) in the binary B. The sign of each B_i is typically determined by $(-\dot{W})$, because in the range of W values we consider, the second term in the brackets is smaller than the first one. Thus, $B_1 < 0$ and $B_2 > 0$. In these circumstances:

(i) Any trajectory originating above the upper separatrix with $\varphi = 0$ will arrive at $\varphi = \pi$ with the Hamiltonian value decreased by $|B_1|$ (i.e. with $B_1 < 0$ added) and migrate away from the separatrix (in top panel of Fig. 4 – upwards). Capture does not occur.

(ii) A trajectory departing from a phase plane point below the lower separatrix, say $J \lesssim W/(1+C)$ and $\varphi = \pi$, will arrive at the vicinity of $\varphi = 0$ with the Hamiltonian value increased by B_2, hence, inside the libration zone. But then the motion below the upper separatrix decreases the Hamiltonian value by $|B_1|$, which means a drift outwards the libration zone. The net effect

$$B_1 + B_2 = 24\,\dot{W}\sqrt{\frac{2\beta}{\alpha}}\, W^5, \tag{86}$$

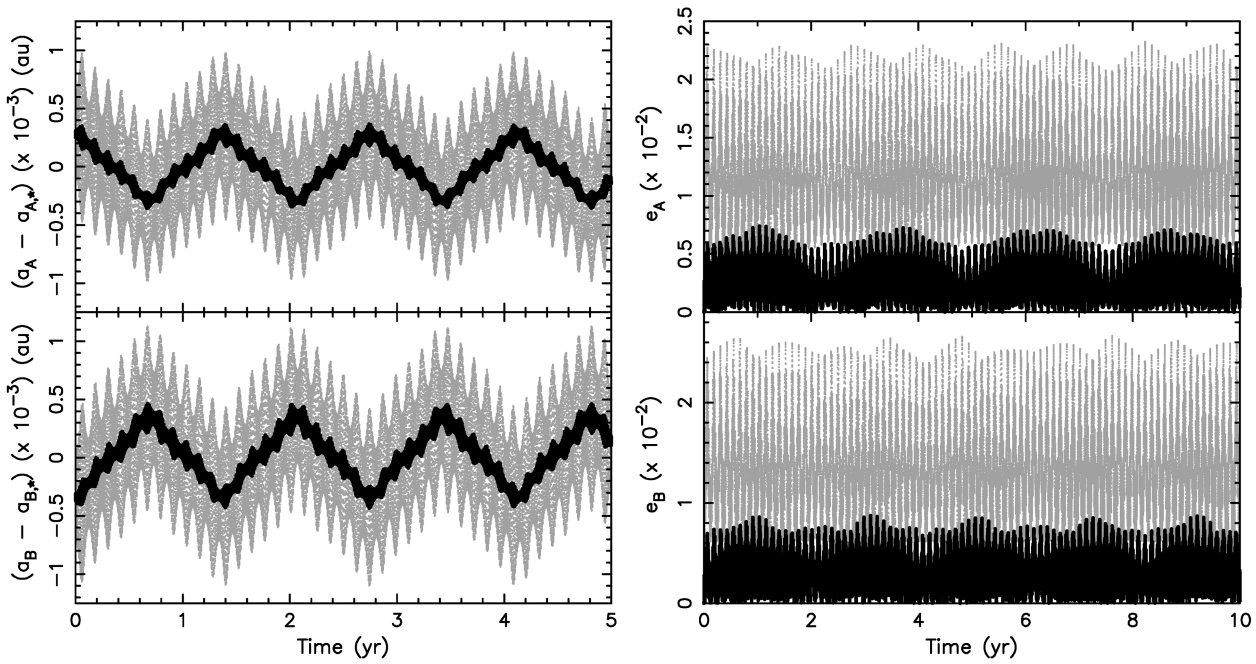

Figure 9. The same as in Fig. 7, but now for a 2+2 system with the same masses and orbital periods as in the KIC 4247791 system: $m_1 = 1.70\ \mathrm{M}_\odot$, $m_2 = 1.54\ \mathrm{M}_\odot$, $m_3 = 1.46\ \mathrm{M}_\odot$, $m_4 = 1.35\ \mathrm{M}_\odot$, $P_\mathrm{A} = 4.100\,871$ d, and $P_\mathrm{B} = 4.049\,732$ d (see Lehmann et al. 2012). The reference semimajor axes are now $a_{\mathrm{A},\star} \simeq 0.073\,9404$ au and $a_{\mathrm{B},\star} \simeq 0.070\,4749$ au. The relative orbit has been given a period $P = 45$ d and eccentricity $e = 0.1$. Compactness of the system now makes short-period effects stronger, exciting osculating eccentricities (grey symbols) up to few per cent. The mean eccentricities (black symbols) are about an order of magnitude smaller, but non-zero.

inherits the sign of $\dot{W}$, so the Hamiltonian value per one cycle is decreased. Accordingly, after a short visit to the libration zone, the trajectory continues the drift upwards, like in the case (i). Again, capture does not occur.

(iii) For the same reasons as in case (ii), a trajectory with the origin at the outskirts of the libration zone (but inside it) will exit upwards.

Thus, when the dissipation decreases W, the capture into permanent 1:1 resonance does not occur in our model.

The case of $\dot{W} > 0$ may eventually lead to a capture with probability (Henrard 1982)

$$P_\mathrm{c} = \frac{B_1 + B_2}{B_1}, \tag{87}$$

which is fairly small. For a completely symmetric system with $e = 0$, and $W < 0.3$, it is below 0.02, and scales as W^5. Moreover, it is difficult to identify a proper physical scenario resulting in the increase of W.

In a similar manner, we have verified that the case of mass transfer between the components of one of the binaries (this scenario strictly adheres to the assumptions of the Henrard's model) results in B_1 and B_2 having opposite signs, with a small sum $B_1 + B_2$, that leads to the low probability of capture, proportional to W^5. Thus, capture in the resonance caused by the variation of μ_A or μ_B is also unlikely, although it might happen for some particular values of $\dot{\mu}_A + \dot{\mu}_\mathrm{B}$.

7 CONCLUSIONS

In the present work, we dealt with a resonant configuration of a quadruple stellar system in 2+2 architecture. In particular, we considered the case where the mean orbital periods P_A and P_B are very close to each other hence constituting 1:1 mean motion resonance. As typical in orbital mechanics, the resonant problem has been reduced to 1-degree Hamiltonian case allowing semi-analytical estimates of resonant width and several other interesting parameters. A comparison with direct numerical integration of the complete problem allowed us to justify the simplified model. We found that phase space occupied by the 1:1 resonance in 2+2 quadruple shrinks to very small volume for realistic ratio of the outer orbit period P and periods P_A or P_B of the binaries. Additionally, adiabatic changes of P_A or P_B driving them towards the resonant configuration result in only very small probability of capture. Therefore, number of existing 2+2 systems in the 1:1 resonance is expected to be very small.

In spite of the negative result, techniques and tools developed here are suitable starting point for the next paper where we plan to deal with the more complicated situations of the first-order resonances 2:1 and 3:2 between P_A and P_B. As explained in the Introduction, there are at least two observed quadruple systems that were suggested to be locked in the 3:2 case. With the appropriate theoretical tools available, we will be able to consider necessary parametric conditions for the resonance to exist and likelihood of the system to be captured in this state.

ACKNOWLEDGEMENTS

This work was partly funded through the research grant P209-13-01308S of the Czech Science Foundation. We thank the anonymous reviewer for valuable comments, especially for signalling the error in equation (10) of Vokrouhlický (2016), reproduced in the first version of the this paper.

REFERENCES

Beust H., 2003, A&A, 400, 1129
Borkovits T., Erdi B., Forgács-Dajka E., Kovács T., 2003, A&A, 398, 1091
Borkovits T., Csizmadia Sz., Forgács-Dajka E., Hegedüs T., 2011, A&A, 528, A53
Borkovits T., Hajdu T., Sztakovics J., Rappaport S., Levine A., Bíró I. B., Klagyivik P., 2016, MNRAS, 455, 4136
Breiter S., Vokrouhlický D., 2015, MNRAS, 449, 1691
Brown E. W., 1936a, MNRAS, 97, 56
Brown E. W., 1936b, MNRAS, 97, 62
Brown E. W., 1936c, MNRAS, 97, 116
Brown E. W., 1937, MNRAS, 97, 388
Cagaš P., Pejcha O., 2012, A&A, 544, L3
Cohen C. J., Lyddane R. H., 1981, Celest. Mech., 25, 221
Garfinkel B., 1970, Celest. Mech., 2, 359
Hamers A. S., Lai D., 2017, MNRAS, 470, 1657
Hamers A. S., Portegies Zwart S. F., 2016, MNRAS, 459, 2827
Hamers A. S., Perets H. B., Antonini F., Portegies Zwart S. F., 2015, MNRAS, 449, 4221
Harrington R. S., 1969, Celest. Mech., 1, 200
Henrard J., 1982, Celest. Mech., 27, 3
Kołaczkowski Z., Mennickent R. E., Rivinius T., Pietrzyński G., 2013, MNRAS, 429, 2852
Lehmann H., Zechmeister M., Dreizler S., Schuh S., Kanzler R., 2012, A&A, 541, A105
Mardling R. A., Aarseth S. J., 2001, MNRAS, 321, 398
Milani A., Nobili A. M., 1983, Celest. Mech., 31, 241
Nemravová J. A. et al., 2016, A&A, 594, A55
Ofir A., 2008, IBVS, 5868
Pawlak M. et al., 2013, AcA, 63, 323
Pejcha O., Antognini J. M., Shappee B. J., Thompson T. A., 2013, MNRAS, 435, 943
Pribulla T., Baluďanský D., Dubovský P., Kudzej I., Parimucha Š., Siwak M., Vaňko M., 2008, MNRAS, 390, 798
Rappaport S., Deck K., Levine A., Borkovits T., Carter J., El Mellah I., Sanchis-Ojeda R., Kalomeni B., 2013, ApJ, 768, 33
Rappaport S. et al., 2017, MNRAS, 467, 2160
Riddle R. L. et al., 2015, ApJ, 799, 4
Rivinius T., Mennickent R. E., Kołaczkowski Z., 2011, in Neiner C. et al., eds, Active OB Stars: Structure, Evolution, Mass Loss and Critical Limits. Cambridge Univ. Press, Cambridge, p. 541
Söderhjelm S., 1975, A&A, 42, 229
Söderhjelm S., 1982, A&A, 107, 54
Sterzik M. F., Tokovinin A . , A&A, 384, 1030
Tokovinin A., 2008, MNRAS, 389, 925
Tokovinin A., 2014, AJ, 147, 87
Vokrouhlický D., 2016, MNRAS, 461, 3964
Zasche P., Uhlař R., 2013, MNRAS, 429, 3472
Zasche P., Uhlař R., 2016, A&A, 588, A121

APPENDIX A: SHORT PERIOD PERTURBATIONS

Linear, short period perturbations, albeit of low accuracy, can be useful for the order of magnitude estimation, or help to establish initial conditions for the numerical integration related to the specified mean orbit of the secular system. The expressions below are derived from the generating function

$$\mathcal{S} = \mathcal{S}_1 + \mathcal{S}_2, \tag{A1}$$

where the term $\mathcal{S}_1$ is given by equation (33) and $\mathcal{S}_2$ by equation (42). It is worth noting that $\mathcal{S}_1 = \varepsilon^3 \mathcal{S}_2$, so the short periodic terms resulting from the motion on the principal orbit should dominate.

Then, for any function of canonical variables, its osculating vales Y_o are, approximately, given by the Poisson bracket with $\mathcal{S}$

$$Y_\mathrm{o} = Y + \{Y, \mathcal{S}\} = Y + \delta Y, \tag{A2}$$

where the expressions to the right are functions of the mean variables (solution of the system defined by $\mathcal{K}$). Although using a simple sum (A1) we ignore the coupling term $\{\mathcal{S}_1, \mathcal{S}_2\}$, the loss is negligible (of the order ε^{10}).

Once the Poisson bracket in (A2) has been evaluated (but not earlier !), we can set the mean eccentricities $e_\mathrm{A} = e_\mathrm{B} = 0$, according to the adopted model.

A1 Binaries a and b

Let ν refers to subscript A or B. Then the short periodic perturbations in the semi-axes are

$$\delta a_\nu = c_\nu \frac{3\, n^2 a^3\, a_\nu}{2\, n_\nu^2 R^3} \cos 2(F - \lambda_\nu), \tag{A3}$$

where $c_\mathrm{A} = \mu$ and $c_\mathrm{B} = (1 - \mu)$. For the mean longitudes,

$$\delta\lambda_\nu = - c_\nu \frac{n}{n_\nu} \left(\frac{f - l + e \sin f}{\eta^3} - \frac{21}{8} \frac{n a^3}{n_\nu R^3} \sin 2(F - \lambda_\nu) \right), \tag{A4}$$

the first term in the bracket, resulting from $\mathcal{S}_2$ should generally dominate, but for very small and/high eccentricity e, the second term may become important. This is because the first term strictly speaking vanishes for $e = 0$, and the second term may be strongly amplified at the pericentre for large e value. It is of interest to note that the first, long-period, term in equation (A4) has been extensively used for analysis of eclipse time variations in hierarchical triple systems (see e.g. Söderhjelm 1975, 1982; Borkovits et al. 2003, 2011, 2016; Rappaport et al. 2013). The second term has been overlooked and only recently briefly mentioned in Nemravová et al. (2016). Here, we give, for the first time, its formal derivation.

Due to the peculiarities of a perturbed small eccentricity orbit (e.g. Cohen & Lyddane 1981), the perturbations in eccentricities and longitudes of pericentres must be computed indirectly, through non-singular variables

$$k_\nu = e_\nu \cos \varpi_\nu, \qquad h_\nu = e_\nu \sin \varpi_\nu. \tag{A5}$$

There we find

$$k_{\mathrm{o},\nu} = \delta k_\nu = \frac{c_\nu}{4} \frac{n^2 a^3}{n_\nu^2 R^3} (9 \cos(2F - \lambda_\nu) - 2 \cos \lambda_\nu + \cos(2F - 3\lambda_\nu)), \tag{A6}$$

$$h_{\mathrm{o},\nu} = \delta h_\nu = \frac{c_\nu}{4} \frac{n^2 a^3}{n_\nu^2 R^3} (9 \sin(2F - \lambda_\nu) - 2 \sin \lambda_\nu \sin(2F - 3\lambda_\nu)), \tag{A7}$$

and the osculating eccentricities

$$e_{\mathrm{o},\nu} = \sqrt{k_{\mathrm{o},\nu}^2 + h_{\mathrm{o},\nu}^2} = = \frac{c_\nu n^2 a^3}{2\sqrt{2}\, n_\nu^2 R^3} \sqrt{43 - 20 \cos 2(F - \lambda_\nu) + 9 \cos 4(F - \lambda_\nu)}. \tag{A8}$$

The osculating longitudes of pericentres actually evolve quickly – the apsides rotate at the rate of n_ν, as seen from

$$\tan \varpi_\nu = \frac{h_{\mathrm{o},\nu}}{k_{\mathrm{o},\nu}}. \tag{A9}$$

Osculating mean anomalies merely oscillate around 0 or π, as found from

$$l_{\mathrm{o},\nu} = \lambda_\nu - \varpi_\nu + \delta\lambda_\nu. \tag{A10}$$

A2 Principal orbit

Perturbations in the semi-axis of the principal orbit are

$$\delta a = d_{a,\mathrm{A}} + d_{a,\mathrm{B}}, \tag{A11}$$

$$d_{a,\nu} = \mu_\nu(1-\mu_\nu)\frac{n a_\nu^2 a^2}{2 n_\nu R^3}\left[\frac{n_\nu}{n}\left(1-\left(\frac{R}{a\eta}\right)^3\right) - \frac{3a^2\eta}{R^2}\cos 2(F-\lambda_\nu) + \frac{9ea\sin f}{2R\eta}\sin 2(F-\lambda_\nu)\right] \tag{A12}$$

$$= -\mu_\nu(1-\mu_\nu)\frac{3n a_\nu^2}{2 n_\nu a}\cos 2(\lambda-\lambda_\nu) + O(e), \tag{A13}$$

where equation (A13) can be used for sufficiently small eccentricity of the principal orbit. Short periodic perturbations in the mean longitude are

$$\delta\lambda = d_{\lambda,\mathrm{A}} + d_{\lambda,\mathrm{B}}, \tag{A14}$$

$$d_{\lambda,\nu} = \mu_\nu(1-\mu_\nu)\frac{3a_\nu^2}{4a^2\eta^4}\left[f - l + \left(\frac{3+\eta}{4} + \frac{1}{1+\eta}\right)e\sin f + \frac{e^2\sin 2f}{2(1+\eta)} + \frac{e^3\sin 3f}{12(1+\eta)} - \frac{n a^3\eta^3}{n_\nu R^3}\left(3\eta\left(1-\frac{a\eta(R-a\eta^2)}{2R^2(1+\eta)}\right)\sin 2(F-\lambda_\nu) + \frac{(R+a\eta^2)e\sin f}{R(1+\eta)}\cos 2(F-\lambda_\nu)\right)\right] \tag{A15}$$

$$= -\mu_\nu(1-\mu_\nu)\frac{9n a_\nu^2}{4 n_\nu a^2}\sin 2(\lambda-\lambda_\nu) + O(e). \tag{A16}$$

For the eccentricity and the longitude of pericentre, we find

$$\delta e = d_{e,\mathrm{A}} + d_{e,\mathrm{B}}, \tag{A17}$$

$$d_{e,\nu} = -\mu_\nu(1-\mu_\nu)\frac{a_\nu^2}{4a^2 e}\left[\frac{1}{\eta} - \frac{a^3\eta^2}{R^3} + \frac{3n a^4\eta}{4 n_\nu R^4}\left(4\left(1-\frac{R}{a}\right)\cos 2(F-\lambda_\nu) \frac{1}{\eta} - e\cos(F-2\lambda_\nu+\varpi) + 5e\cos(3F-2\lambda_\nu-\varpi)\right)\right], \tag{A18}$$

and

$$\delta\varpi = d_{\varpi,\mathrm{A}} + d_{\varpi,\mathrm{B}}, \tag{A19}$$

$$d_{\varpi,\nu} = -\mu_\nu(1-\mu_\nu)\frac{3a_\nu^2}{4a^2\eta^4}\left[f - l + \left(\frac{1}{e} + \frac{3e}{4}\right)\sin f + \frac{1}{2}\sin 2f + \frac{e}{12}\sin 3f - \frac{n a^3\eta^3}{n_\nu R^3}\left(\frac{3}{4}\sin 2(F-\lambda_\nu) - \frac{1}{8}\sin 2(\lambda_\nu-\varpi) + \frac{5}{8}\sin(4F-2\lambda_\nu-2\varpi) - \frac{1}{4e}\sin(F-2\lambda_\nu+\varpi) + \frac{7}{4e}\sin(3F-2\lambda_\nu-\varpi)\right)\right] \tag{A20}$$

The above expressions for δe and $\delta\varpi$ are valid only for sufficiently large eccentricity values (i.e. as long as the negative values of the osculating eccentricity do not appear). For small mean eccentricities, non-singular variables

$$K = e\cos\varpi, \qquad H = e\sin\varpi, \tag{A21}$$

should be used. Then, assuming the mean variables $H = K = 0$, we obtain

$$K_\mathrm{o} = d_{K,\mathrm{A}} + d_{K,\mathrm{B}}, \qquad H_\mathrm{o} = d_{H,\mathrm{A}} + d_{H,\mathrm{B}}, \tag{A22}$$

with

$$d_{K,\nu} = \mu_\nu(1-\mu_\nu)\frac{3a_\nu^2}{4a^2}\left[\cos\lambda - \frac{n}{4n_\nu}\left(7\cos(3\lambda-2\lambda_\nu) + \cos(\lambda-2\lambda_\nu)\right)\right], \tag{A23}$$

$$d_{H,\nu} = \mu_\nu(1-\mu_\nu)\frac{3a_\nu^2}{4a^2}\left[\sin\lambda - \frac{n}{4n_\nu}\left(7\sin(3\lambda-2\lambda_\nu) - \sin(\lambda-2\lambda_\nu)\right)\right]. \tag{A24}$$

All the perturbation formulas can also be used as an analytical filter of the observed elements. The approximate values of the mean elements result from the subtraction

$$Y = Y_\mathrm{o} - \delta Y, \tag{A25}$$

where osculating values are substituted into the right-hand side.

APPENDIX B: SECULAR EVOLUTION OF INNER ECCENTRICITIES

Secular interaction of the two binary systems A and B may be solved analytically in the crudest approximation of nearly circular and coplanar orbits. While very restrictive, it is useful to understand some of our results in Section 5.

Denote $\boldsymbol{e}_\mathrm{A}$, $\boldsymbol{e}_\mathrm{B}$, and $\boldsymbol{e}$ vectors pointing to the pericentre of the orbits A, B and mutual orbit with lengths equal to the appropriate eccentricities e_A, e_B, and e. Such normalized Laplace vectors represent half of Milankovitch-type non-singular variables used by Vokrouhlický (2016) for description of the secular evolution of the 2+2 quadruple systems. Retaining only the linearly-averaged quadrupole ($n = 2$) and octupole ($n = 3$) interaction terms $\mathcal{H}_\mathrm{int}$ in equation (23), we obtain (see Vokrouhlický 2016, for details; $\nu = \mathrm{A}$ or B as before)

$$\frac{\mathrm{d}\boldsymbol{e}_\nu}{\mathrm{d}t} = \omega_\nu\,\boldsymbol{k}\times\left[\boldsymbol{e}_\nu - \frac{2\gamma_\nu}{\eta^2}\boldsymbol{e}\right], \tag{B1}$$

where $\boldsymbol{k}$ is the normal unit vector to the orbital plane of the quadruple system. We also denoted (as usual $\eta = \sqrt{1-e^2}$, $c_\mathrm{A} = \mu$, and $c_\mathrm{B} = 1-\mu$)

$$\omega_\nu = \frac{3}{4}\frac{n^2}{n_\nu}\frac{c_\nu}{\eta^3}, \tag{B2}$$

and

$$\gamma_\nu = \frac{5}{8}(1-2\mu_\nu)\left(\frac{a_\nu}{a}\right). \tag{B3}$$

Assuming small inner eccentricities, the quadratic terms in e_A and e_B have been neglected in the right-hand sides of equations (B1). For exactly equal-mass binaries A and B, thence $1-2\mu_\mathrm{A} = 1-2\mu_\mathrm{B} = 0$, these equations are autonomous and provide a trivial time evolution of $\boldsymbol{e}_\mathrm{A}$ and $\boldsymbol{e}_\mathrm{B}$: a constant circulation

in the plane normal to $\boldsymbol{k}$ with frequencies $\omega_{\rm A}$ and $\omega_{\rm B}$. A small mismatch in masses of the binaries activates the role of the octupole interaction and makes time evolution of $\boldsymbol{e}_{\rm A}$ and $\boldsymbol{e}_{\rm B}$ coupled to the time evolution of their relative-orbit pericentre vector $\boldsymbol{e}$. Neglecting terms of the order of eccentricities $e_{\rm A}$ and $e_{\rm B}$ in the right hand side of $\mathrm{d}\boldsymbol{e}/\mathrm{d}t$, we conclude that $\boldsymbol{e}$ steadily circulates about $\boldsymbol{k}$ with frequencies $\omega_{\rm AB}$, whose quadrupole approximation provides

$$\omega_{\rm AB} \simeq \frac{3}{4}\frac{n}{a^2\eta^4}\left[\mu_{\rm A}\left(1-\mu_{\rm A}\right)a_{\rm A}^2+\mu_{\rm B}\left(1-\mu_{\rm B}\right)a_{\rm B}^2\right]. \tag{B4}$$

In order to proceed with secular eccentricity solution of the inner systems A and B, we set $\boldsymbol{k}=(0,0,1)$ and $\boldsymbol{e}=(K,H,0)$, where $K=e\cos\varpi$ and $H=e\sin\varpi$. As mentioned above e is constant and $\varpi=\omega_{\rm AB}t+\varpi_0$. Denoting $\boldsymbol{e}_\nu=(k_\nu,h_\nu,0)$, we now write equation (B1) in the following form:

$$\frac{\mathrm{d}k_\nu}{\mathrm{d}t}=-\omega_\nu\left[h_\nu-2\frac{e\gamma_\nu}{\eta^2}\sin\varpi\right], \tag{B5}$$

$$\frac{\mathrm{d}h_\nu}{\mathrm{d}t}=\omega_\nu\left[k_\nu-2\frac{e\gamma_\nu}{\eta^2}\cos\varpi\right]. \tag{B6}$$

This is a simple system describing two-dimensional forced harmonic oscillator with proper frequency ω_ν. Assuming, in particular, initial conditions at origin, notably $\boldsymbol{e}_\nu=(0,0,0)$ for $t=0$, we obtain

$$k_\nu(t)=-e_{\star,\nu}\left[\cos\left(\omega_\nu t+\varpi_0\right)-\cos\varpi\right], \tag{B7}$$

$$h_\nu(t)=-e_{\star,\nu}\left[\sin\left(\omega_\nu t+\varpi_0\right)-\sin\varpi\right], \tag{B8}$$

where

$$e_{\star,\nu}=2\frac{e\gamma_\nu}{\eta^2}\frac{1}{1-\frac{\omega_{\rm AB}}{\omega_\nu}}. \tag{B9}$$

This is the forced eccentricity by the presence of the octupole term in the interaction of systems A and B, replacing the zero-eccentricity stationary state in the quadrupole model.

From equations (B7) and (B8), we easily obtain secular evolution of the system A eccentricity

$$e_\nu(t)=\sqrt{2}e_{\star,\nu}\sqrt{1-\cos\left(\omega_\nu-\omega_{\rm AB}\right)t}. \tag{B10}$$

The eccentricity reaches a maximum $2e_{\star,\nu}$. A consistency of the solution obviously requires that this quantity remains small.

This paper has been typeset from a TEX/LATEX file prepared by the author.